

การหาปัจจัยที่เหมาะสมในการสร้างภาพสมองด้วยวิธีไอเอสอีเอ็มและเอฟบีทีที่ระดับต่างๆ
ของความเข้มข้นของความแรงกัมมันตภาพรังสีด้วยเครื่องสเปค



นางสาวเม พิวิ ชิน เตง

จุฬาลงกรณ์มหาวิทยาลัย

CHULALONGKORN UNIVERSITY

บทคัดย่อและแฟ้มข้อมูลฉบับเต็มของวิทยานิพนธ์ตั้งแต่ปีการศึกษา 2554 ที่ให้บริการในคลังปัญญาจุฬาฯ (CUIR)
เป็นแฟ้มข้อมูลของนิสิตเจ้าของวิทยานิพนธ์ ที่ส่งผ่านทางบัณฑิตวิทยาลัย

The abstract and full text of theses from the academic year 2011 in Chulalongkorn University Intellectual Repository (CUIR)
are the thesis authors' files submitted through the University Graduate School.

วิทยานิพนธ์นี้เป็นส่วนหนึ่งของการศึกษาตามหลักสูตรปริญญาวิทยาศาสตรมหาบัณฑิต

สาขาวิชาอายุรศาสตร์ ภาควิชารังสีวิทยา

คณะแพทยศาสตร์ จุฬาลงกรณ์มหาวิทยาลัย

ปีการศึกษา 2559

ลิขสิทธิ์ของจุฬาลงกรณ์มหาวิทยาลัย

OPTIMIZATION OF ACTIVITY CONCENTRATION AND RECONSTRUCTION
PARAMETERS OF OSEM AND FBP METHODS IN BRAIN SPECT IMAGING

Miss May Phyu Zin Thein



A Thesis Submitted in Partial Fulfillment of the Requirements
for the Degree of Master of Science Program in Medical Imaging
Department of Radiology
Faculty of Medicine
Chulalongkorn University
Academic Year 2016
Copyright of Chulalongkorn University

Thesis Title	OPTIMIZATION OF ACTIVITY CONCENTRATION AND RECONSTRUCTION PARAMETERS OF OSEM AND FBP METHODS IN BRAIN SPECT IMAGING
By	Miss May Phyu Zin Thein
Field of Study	Medical Imaging
Thesis Advisor	Associate Professor Anchali Krisanachinda, Ph.D.
Thesis Co-Advisor	Kitiwat Khamwan, Ph.D.

Accepted by the Faculty of Medicine, Chulalongkorn University in Partial
Fulfillment of the Requirements for the Master's Degree

..... Dean of the Faculty of Medicine
(Professor Suttipong Wacharasindhu, M.D.)

THESIS COMMITTEE

..... Chairman
(Associate Professor Tawatchai Chaiwatanarat, M.D.)

..... Thesis Advisor
(Associate Professor Anchali Krisanachinda, Ph.D.)

..... Thesis Co-Advisor
(Kitiwat Khamwan, Ph.D.)

..... Examiner
(Associate Professor Supatporn Tepmongkol, M.D.)

..... External Examiner
(Professor Franco Milano, Ph.D.)

เม พิว ชิน เตง : การหาปัจจัยที่เหมาะสมในการสร้างภาพสมองด้วยวิธี โอเอสเอ็มและเอพีบีทีที่ระดับต่างๆของความเข้มข้นของ ความแรงกัมมันตภาพรังสีด้วยเครื่องสเปค (OPTIMIZATION OF ACTIVITY CONCENTRATION AND RECONSTRUCTION PARAMETERS OF OSEM AND FBP METHODS IN BRAIN SPECT IMAGING) อ.ที่ปริกษาวิทยานิพนธ์หลัก: อัญชลี กฤษณ จินดา, อ.ที่ปริกษาวิทยานิพนธ์ร่วม: กิติวัฒน์ คำวัน, หน้า.

การตรวจภาพสมองด้วยเครื่องสเปคเป็นการตรวจทางเวชศาสตร์นิวเคลียร์เพื่อดูการไหลเวียนของโลหิตในสมองรวมไปถึงความผิดปกติของสมองส่วนต่างๆ แต่ปัญหาสำคัญที่อาจพบได้จากการตรวจนี้คือเมื่อผู้ป่วยได้รับการฉีดสารเภสัชรังสีที่มีความแรงรังสีต่ำ ซึ่งถึงแม้จะเป็นการช่วยลดปริมาณรังสีให้แก่ผู้ป่วย แต่อาจจะทำให้คุณภาพของภาพลดลงเนื่องจากค่านับวัดลดลงและอาจส่งผลกระทบต่อการวินิจฉัยโรค งานวิจัยนี้จึงมีวัตถุประสงค์เพื่อหาค่าปัจจัยที่เหมาะสมสำหรับการตรวจภาพสมองด้วยสเปคจากการสารเภสัชรังสีที่มีความเข้มข้นแตกต่างกัน โดยเป็นการศึกษาในหุ่นจำลองสมองชนิด Hoffman ซึ่งทำการผสมสารเภสัชรังสีเทคนิคเนียมเปอร์เทคนิค ($^{99m}\text{TcO}_2$) ในของเหลวและเติมใส่ในหุ่นจำลองให้มีความแรงรังสีที่แตกต่างกัน 3 ค่า คือ 55.5 เมกกะเบคเคอเรล, 111 เมกกะเบคเคอเรล และ 165.5 เมกกะเบคเคอเรล สำหรับจำลองความแรงของรังสีปริมาณต่ำ ปานกลางและสูง ในสมองตามลำดับ ทำการเก็บข้อมูลภาพสเปคของหุ่นจำลองโดยใช้เครื่องสเปค/ซีทีของบริษัทซีเมนส์รุ่น Symbia True Point T6 SPECT/CT และนำข้อมูลมาทำการสร้างภาพด้วยอัลกอริทึมที่แตกต่างกัน 2 วิธี คือ การสร้างภาพแบบอิตเทอร์เรชั่น ซึ่งจะปรับเปลี่ยนค่าพารามิเตอร์ที่เกี่ยวข้องกับจำนวนครั้งโดยค่าซับเซตคองที่ และแบบฟิลเตอร์แบ็คโปรเจกชันซึ่งจะปรับเปลี่ยนค่า Cut-off frequency และลำดับของฟิลเตอร์ชนิดบัตเตอร์เวิร์ธ เปรียบเทียบคุณภาพของภาพทั้งสองวิธีทั้งในเชิงปริมาณจากการหาเปอร์เซ็นต์คอนทราสและค่าความแปรปรวนในเกรย์แมตเตอร์และไวต์แมตเตอร์ และในเชิงคุณภาพจากการให้คะแนนของแพทย์เวชศาสตร์นิวเคลียร์ 2 ท่าน เพื่อหาค่าพารามิเตอร์ที่เหมาะสมจากการสร้างภาพทั้งสองวิธี

ผลการวิจัยพบว่า ค่าพารามิเตอร์ที่เหมาะสมสำหรับการสร้างภาพแบบอิตเทอร์เรชั่นสำหรับความแรงของรังสีปริมาณต่ำ ซึ่งมีความเข้มข้น 46 กิโลเบคเคอเรลต่อซีซี คือ 8 อิตเทอร์เรชั่นและ 8 ซับเซต มีค่าเปอร์เซ็นต์คอนทราสและค่าความแปรปรวนเท่ากับ 66.00% และ 14.60 ตามลำดับ คะแนนการประเมินคุณภาพของภาพโดยแพทย์มีค่าเท่ากับ 12 สำหรับ ความแรงของรังสีปริมาณปานกลาง ซึ่งมีความเข้มข้น 92 กิโลเบคเคอเรลต่อซีซี ค่าพารามิเตอร์ที่เหมาะสมคือ 10 อิตเทอร์เรชั่นและ 8 ซับเซต มีค่าเปอร์เซ็นต์คอนทราสและค่าความแปรปรวนเท่ากับ 78.00% และ 14.00 ตามลำดับ ได้คะแนนจากการประเมินคุณภาพของภาพโดยแพทย์เท่ากับ 13 และพารามิเตอร์ที่เหมาะสมสำหรับความแรงของรังสีปริมาณสูง ซึ่งมีความเข้มข้น 138 กิโลเบคเคอเรลต่อซีซี คือ 12 อิตเทอร์เรชั่นและ 8 ซับเซต มีค่าเปอร์เซ็นต์คอนทราสและค่าความแปรปรวนเท่ากับ 84.00% และ 13.60 ตามลำดับ คะแนนจากการประเมินคุณภาพของภาพ โดยแพทย์เท่ากับ 14 ซึ่งในทุกความเข้มข้นจะกำหนดค่า FWHM ของฟิลเตอร์แบบเกาส์เซียนเท่ากับ 5 มิลลิเมตร และค่าสัมประสิทธิ์การลดลงแบบเชิงเส้นของ Chang's method เท่ากับ 0.12 ซม.⁻¹ สำหรับการสร้างภาพแบบฟิลเตอร์แบ็คโปรเจกชัน ใช้ฟิลเตอร์แบบบัตเตอร์เวิร์ธและค่าสัมประสิทธิ์การลดลงแบบเชิงเส้นของ Chang's method เท่ากับ 0.14 ซม.⁻¹ พบว่าค่า cut-off frequency ที่เหมาะสมสำหรับ ความแรงของรังสีปริมาณต่ำ มีค่าเท่ากับ 0.35 cycles/pixel โดยให้ค่าเปอร์เซ็นต์คอนทราสและค่าความแปรปรวนเท่ากับ 52.92% และ 11.80 แพทย์ทั้งสองท่านให้คะแนนคุณภาพของภาพอยู่ที่ 12 คะแนน ค่า cut-off frequency ที่เหมาะสมสำหรับ ความแรงของรังสีปริมาณปานกลางมีค่าเท่ากับ 0.45 cycles/pixel โดยให้ค่าเปอร์เซ็นต์คอนทราสและค่าความแปรปรวนเท่ากับ 62.19% และ 11.00 แพทย์ทั้งสองท่านให้คะแนนคุณภาพของภาพอยู่ที่ 10 คะแนน ส่วน cut-off frequency ที่เหมาะสมสำหรับ ความแรงของรังสีปริมาณสูงมีค่าเท่ากับ 0.45 cycles/pixel โดยให้ค่าเปอร์เซ็นต์คอนทราสและค่าความแปรปรวนเท่ากับ 68.61% และ 10.70 ตามลำดับ แพทย์ทั้งสองท่านให้คะแนนคุณภาพของภาพอยู่ที่ 13 คะแนน

จากผลการวิจัยนี้สรุปได้ว่าถึงแม้ภาพสเปคของสมองที่ให้ค่าความแรงของรังสีปริมาณต่ำแต่สามารถปรับปรุงคุณภาพของภาพให้ดีขึ้นได้เมื่อใช้ค่าพารามิเตอร์ในการสร้างภาพที่เหมาะสม โดยเฉพาะอย่างยิ่งเมื่อใช้สารเภสัชรังสีที่มีความแรงรังสีต่ำ และเป็นการช่วยลดปริมาณรังสีให้แก่ผู้ป่วยอีกเช่นเดียวกัน การสร้างภาพแบบอิตเทอร์เรชั่นจะมีความเหมาะสมมากกว่าแบบฟิลเตอร์แบ็คโปรเจกชัน

ภาควิชา รังสีวิทยา

สาขาวิชา ฉายาเวชศาสตร์

ปีการศึกษา 2559

ลายมือชื่อนิติลิต

ลายมือชื่อ อ.ที่ปริกษาหลัก

ลายมือชื่อ อ.ที่ปริกษาร่วม

5874060030 : MAJOR MEDICAL IMAGING

KEYWORDS: SPECT/CT / FBP AND OSEM / RECONSTRUCTION PARAMETERS / OPTIMIZATION

MAY PHYU ZIN THEIN: OPTIMIZATION OF ACTIVITY CONCENTRATION AND RECONSTRUCTION PARAMETERS OF OSEM AND FBP METHODS IN BRAIN SPECT IMAGING. ADVISOR: ASSOC. PROF. ANCHALI KRISANACHINDA, Ph.D., CO-ADVISOR: KITIWAT KHAMWAN, Ph.D., pp.

Brain SPECT imaging is a nuclear medicine study which can detect blood flow and activity in the brain of the patients with neurological and psychiatric disorders. The major problem of brain SPECT imaging is that when the administered activity is low, scanning time is short or counts rate is low, the image quality was reduced and difficult for diagnosis. To compensate for this problem, the optimal reconstruction parameters can be applied to improve the image quality in terms of contrast, noise quantitatively and visual scoring on brain SPECT images. The purpose of this study was to determine the optimal reconstruction parameters of different activity concentration in brain SPECT images by using Hoffman 3-D brain phantom.

Three different activities of $^{99m}\text{TcO}_4$ solution, 55.5-MBq (1.5 mCi)-low activity, 111-MBq (3 mCi) - normal activity, and 165.5-MBq (4.5 mCi)-high activity had been inserted in Hoffman 3D brain phantom for three acquisitions and reconstruct using OSEM with various update numbers and full width at half maximum (FWHM) of Gaussian filter and FBP with various cut-off frequencies and Butterworth filter were applied. The percent contrast and noise of gray and white matter were calculated to determine optimal reconstruction parameters in brain SPECT imaging for quantitative measurement and visual scoring from two nuclear medicine physicians for qualitative analysis. The optimal parameters for 3D-OSEM method in low activity concentration (46 kBq/cc) were 8-iteration and 8-subsets (64-iterative updates), percent contrast and noise were 66.00 % and 14.60 and score of 12, for normal activity concentration (92kBq/cc) were 10-iteration and 8-subsets (80-iterative updates), percent contrast and noise were 78.00 % and 14.00 and score of 13, for high activity concentration (138 kBq/cc) were 12-iteration and 8-subsets (96-iterative updates), percent contrast and noise were 84.00 % and 13.60 and qualitative score of 14 respectively. FWHM of Gaussian filter 5-mm and Chang's attenuation coefficient of 0.12cm^{-1} were fixed for each activity concentration. For FBP reconstruction, low activity concentration (46 kBq/cc), the optimal parameters were 0.35 cycles/pixel, order 10, percent contrast and noise 52.92 % and 11.80 and score of 10. For normal activity concentration (92 kBq/cc) was 0.45 cycles/pixel, order 10, percent contrast and noise were 62.19 % and 11.00 and qualitative score of 10, for high activity concentration (138 kBq/cc), the optimal parameters were 0.45 cycles/pixel, order 10, percent contrast and noise 68.61 % and 10.70 and qualitative score of 13 respectively. Post processing filter of Butterworth filter and Chang's attenuation coefficient of 0.14cm^{-1} were applied for each activity.

In conclusion, the image quality had been determined to obtain the optimal image reconstruction parameters of OSEM and FBP on the low, normal and high activity concentration for Hoffman brain phantom. This study showed that image quality can be improved by optimizing reconstruction parameters especially in low activity concentration to reduce the patient dose. OSEM reconstruction method is the best choice for low counts statistic. These optimizing parameters can be implemented in routine clinical studies.

Department: Radiology

Field of Study: Medical Imaging

Academic Year: 2016

Student's Signature

Advisor's Signature

Co-Advisor's Signature

ACKNOWLEDGEMENTS

This thesis becomes a reality with this kind support and help of many individuals. I would like to show my sincere thanks to all of them. Foremost, I would like to express my sincerest gratitude and deepest appreciation to my advisor Associate Professor Dr. Anchali Krisanachinda, Department of Radiology, Faculty of Medicine, Chulalongkorn University, my major advisor, for her supervision, guidance, constructive comment, encouragement and invaluable advice during the whole study. I attribute the level of my Master degree to her encouragement and effort and without her this thesis, too, would not have been completed or written. I wish to express deepest appreciation to Dr Kitiwat Khamwan and Mr. Panya Pasawang, Medical Imaging Program, Faculty of Medicine, Chulalongkorn University and Section of Nuclear Medicine, Department of Radiology, King Chulalongkorn Memorial Hospital, my co-advisors for their help in the experiment, assistance, invaluable advice and suggestion in this research.

Beside my advisor, I would like to thank the rest of my thesis committee: Associate Professor Dr. Tawatchai Chaiwatanarat, M.D, and Associate Professor Dr. Supatporn Tepmonkol, M.D Nuclear Medicine Division, Department of Radiology, Faculty of Medicine, Chulalongkorn University, for their comments and valuable suggestion to this study. I would like to express my greatly thanks to Associate Professor Dr. Supatporn Tepmonkol, M.D and Dr Maythinee Chantadisai, M.D, Nuclear Medicine Division, Department of Radiology, Faculty of Medicine, Chulalongkorn University, for an instructor in their advice, helpful suggestions and guidance to improve protocol and opinion in image quality in this research. I would like to extremely thank Professor Franco Milano, external examiner, University of Florence, Italy for his constructive comments and valuable suggestion of thesis defense. I would like to greatly thank to medical physicists, nuclear medicine physicians and Radiological Technologists, Section of Nuclear Medicine, King Chulalongkorn Memorial Hospital, Thai Red Cross Society, especially, Mr. Tanawat Sontrapornpol, Mr. Chatchai Navikhacheewin, for their help and suggestions in this study. I am also thankful for all teachers, lecturers and staffs in the Master of Science Program in Medical Imaging, Faculty of Medicine, Chulalongkorn University, for their unlimited teaching of knowledge throughout whole study. I would like to thanks to my friends from MICU 13.

Finally, I would like to thank the Director of Pinlon Hospital, Myanmar, because of his supporting I could study in Chulalongkorn University for two-year Master degree course. Most importantly none of this could have happened without my family, I would like to thank my family; especially my parents, for giving birth to me at the first place and supporting me spiritually throughout my life.

CONTENTS

	Page
THAI ABSTRACT	iv
ENGLISH ABSTRACT.....	v
ACKNOWLEDGEMENTS	vi
CONTENTS.....	vii
LIST OF TABLES	x
LIST OF FIGURES	xii
LIST OF ABBREVIATIONS.....	xv
CHAPTER I.....	1
INTRODUCTION	1
1.1 Background and rationale	1
1.2 Research Objective	2
1.3 Definition.....	2
CHAPTER II.....	4
REVIEW OF RELATED LITERATURE	4
2.1 Theory.....	4
2.1.1 Overview of brain perfusion SPECT.....	4
2.1.2 Clinical Application of Brain Perfusion SPECT	4
2.1.3 Transport and behavior in human brain	4
2.2 Principle of brain SPECT imaging	5
2.3 Photon attenuation	5
2.4 Scatter effect and correction	6
2.5 SPECT/CT	6
2.5.1 Data Acquisition.....	6
2.6 SPECT Reconstruction	7
2.6.1 Filtered back projection.....	7
2.6.2 Iterative Reconstruction	7
2.6.3 Image Filtering	8
2.6.4 SPECT Filtering	8

	Page
2.6.5 Filter characteristics	8
2.6.5.1 Cutoff frequency (f_c) or Critical frequency	8
2.6.5.2 Order	9
2.7 Factors affecting image quality in brain SPECT	9
2.8 Review of related literature	9
CHAPTER III	12
RESEARCH METHODOLOGY.....	12
3.1 Research design	12
3.2 Conceptual framework.....	13
3.3 Research Question	13
3.4 Keywords	13
3.5 The sample	14
3.6 Materials	14
3.6.1 Single Photon Emission Computed Tomography/ Computed Tomography (SPECT/CT)	14
3.6.2 Hoffman 3D Brain Phantom.....	15
3.6.3 Technetium pertechnetate ($^{99m}\text{TcO}_4^-$)	16
3.7 Methods	16
3.7.1 SPECT/CT QC [APPENDIX A].....	16
3.7.2 The preparation of Hoffman 3D Brain Phantom.....	16
3.7.3 SPECT acquisition	16
3.7.4 Reconstruction.....	17
3.7.5 Data analysis on image quality.....	18
3.7.5.1 Quantitative analysis: Percent Contrast and Noise.....	18
3.7.5.2 Qualitative Image Scoring.....	19
3.8 Statistical analysis.....	20
3.9 Data analysis	20
3.10 Ethical Consideration.....	20
3.11 Expected benefits.....	20

LIST OF TABLES

Table	Page
2.1 Results of the VGR analysis using 1000MBq as reference level of activity.....	10
3.1 Parameters for OSEM method.....	17
3.2 Parameters for FBP method.....	17
3.3 Image Quality Criteria	19
4.1 Percent contrast vs number of iteration from 1-15 of low activity concentration	21
4.2 Noise vs number of iteration from 1-15 in GM region of low activity concentration	22
4.3 Percent contrast vs number of iteration from 1-15 of normal activity concentration	22
4.4 Noise vs number of iteration from 1-15 in GM region of normal activity concentration	23
4.5 Percent contrast vs number of iteration from 1-15 of high activity concentration	23
4.6 Noise vs number of iteration from 1-15 in GM region of high activity concentration	24
4.7 Percent contrast vs cut-off frequency for low activity concentration.....	28
4.8 Noise vs cut-off frequency for low activity concentration	28
4.9 Percent contrast vs cut-off frequency for normal activity concentration.....	29
4.10 Noise vs cut-off frequency for normal activity concentration	29
4.11 Percent contrast vs cut-off frequency for high activity concentration.....	30
4.12 Noise vs cut-off frequency for high activity concentration	30
4.13 The strength of agreement between two observers by using ICC	36
4.14 The result of parameters according to qualitative scoring (OSEM).....	40
4.15 The result of parameters according to qualitative scoring	40
4.16 Summary of optimized protocol for each activity concentration (OSEM).....	41
4.17 Summary of optimized protocol for each activity concentration (FBP).....	41

A 1. Daily quality control of CT for one month results.....	55
A 2. Weekly intrinsic uniformity results for one month (October-2016).....	57
A 3. Daily energy peak results for one month (October-2016)	58
A 4. MHR/COR for 180 - degree detector parallel configuration result	60
A 5. MHR/COR for 180- degree detector parallel verification result	60
A 6. Results from 3D-OSEM reconstruction.....	63
A 7. Results from FBP reconstruction	64
A 8. Sensitivity Results for LEUR collimator	65

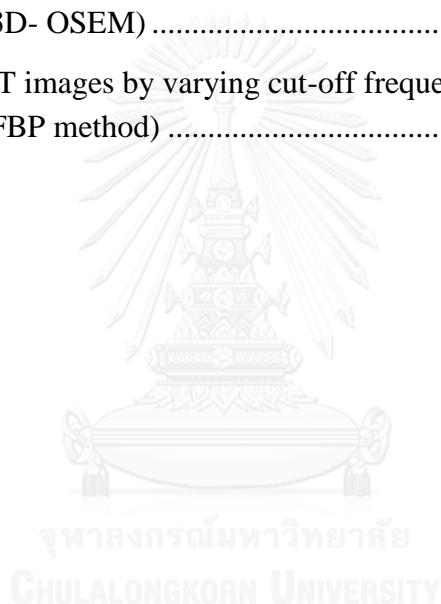


LIST OF FIGURES

Figure	Page
2.1 Effect of varying cut-off frequency of Butterworth filter (0.21 and 0.11) of order $n=10$	8
2.2 Same cut-off frequency and varying order	9
2.3 Relation between iteration no and cut-off frequency as function of % contrast and noise.....	11
3.1 Research Design Model	12
3.2 Conceptual framework.....	13
3.3 SPECT/CT System.....	15
3.4 Hoffman 3D brain phantom (left) and component of brain slabs inside the phantom (right).....	15
3.5 The Hoffman brain phantom acquired with SPECT/CT system	17
3.6 Percent contrast measurement on cerebellum, basal ganglia and vertex regions	18
4.1A The relation between number of iterations and related percent contrast in low activity brain image	25
4.1B The relation between number of iterations and noise in low activity brain image	25
4.2A The relation between iterations number and related percent contrast in normal activity brain image.....	26
4.2B The relation between number of iterations and noise in normal activity brain image	26
4.3A The relation between number of iterations and related percent contrast in high activity brain image.....	27
4.3B The relation between number of iterations and noise in high activity brain image	27
4.4A The relation between cut-off frequency and related percent contrast in low activity.....	31
4.4B The relation between cut-off frequency and noise in low activity.....	31

4.5A The relation between cut-off frequency and related percent contrast in normal activity.....	32
4.5B The relation between cut-off frequency and noise in normal activity.....	32
4.6A The relation between cut-off frequency and related percent contrast in high activity.....	33
4.6B The relation between cut-off frequency and noise in high activity.....	33
4.7 The brain SPECT images by varying number of iterations of 3 activity concentration in OSEM method.....	34
4.8 The brain SPECT images by varying cut-off frequencies of each activity concentration in FBP method.....	35
4.9 Scatter plot of image quality scoring Vs no. of iterations (low activity).....	37
4.10 Scatter plot of image quality scoring Vs no. of iterations (normal activity).....	37
4.11 Scatter plot of image quality scoring Vs no. of iterations (high activity).....	38
4.12 Scatter plot of image quality scoring Vs cut-off frequency (low activity).....	38
4.13 Scatter plot of image quality scoring Vs cut-off frequency (normal activity)....	39
4.14 Scatter plot of image quality scoring Vs cut-off frequency (high activity).....	39
4.15 Images of summarized optimal protocol for each activity concentration.....	44
5.1 Percent contrast and noise comparison between FBP and OSEM reconstruction.....	47
5.2 The images of optimized parameters in low activity concentration (3D-OSEM).....	48
5.3 The images of optimized parameters in normal activity concentration (3D-OSEM).....	49
5.4 The images of optimized parameters in high activity concentration (3D-OSEM).....	50
5.5 The images of optimized parameters in low activity concentration (FBP).....	51
5.6 The images of optimized parameters in normal activity concentration (FBP)...	52
5.7 The images of optimized parameters in hig activity concentration (FBP).....	53
A 1. MHR/COR phantom with 5-point sources.....	61
A 2 . Jaszczak Phantom Scanning.....	63
A 3. Jaszczak Images from OSEM reconstruction.....	64

A 4. Jaszczak Images from FBP reconstruction	65
B 1. The brain SPECT images by varying number of iterations in low activity concentration (3D- OSEM)	67
B 2. The brain SPECT images by varying cut-off frequencies in low activity concentration (FBP method)	68
B 3. The brain SPECT images by varying number of iterations in normal activity concentration (3D- OSEM)	68
B 4. The brain SPECT images by varying cut-off frequencies in normal activity concentration (FBP method)	69
B 5. The brain SPECT images by varying number of iterations in high activity concentration (3D- OSEM)	69
B 6. The brain SPECT images by varying cut-off frequencies in normal activity concentration (FBP method)	70



LIST OF ABBREVIATIONS

%	Percent
3D	Three Dimensions
OSEM	Ordered Subsets Expectation and Maximization
FBP	Filtered Back Projection
FWHM	Full width at half maximum
SD	Standard deviation
CNR	Contrast to Noise Ratio
kVp	Kilo voltage peak
mA	Milliamperere
MBq	Mega Becquerel
kBq	Kilo Becquerel
mCi	Milli Curie
ml	Milliliter
mm	Millimeter
cc	Cubic centimeter
NaI(Tl)	Sodium iodide thallium activated
NEMA	National Electrical Manufacturers Association
PMTs	Photomultiplier tubes

ROI	Region of Interest
VOI	Volume of Interest
SPECT	Single Photon Emission Computed Tomography
CT	Computed Tomography
rCBF	Regional Cerebral Blood Flow
GM	Gray Matter
WM	White Matter
BBB	Blood Brain Barrier
$^{99m}\text{TcO}_4^-$	Technetium Perchnetate
HMPAO	Hexa Methyl Propylene Amine Oxime
ECD	Ethyl Cysteinate Diethyl Ester
F_c	Cut-off Frequency

CHAPTER I

INTRODUCTION

1.1 Background and rationale

Single photon emission computed tomography (SPECT) is a noninvasive imaging technique for tracing radioactive materials in the body and provides three dimensional maps of in vivo radiopharmaceutical distributions. The main benefits are to increase the image contrast due to the reduction in background activity superimposed on object activity, and to increase the accuracy of quantification. The fundamental goal of the tomographic imaging system is to portray the distribution of the radioactivity in the patient more accurately (1).

Brain SPECT imaging is a sophisticated nuclear medicine study which can detect blood flow and activity in the brain of the patients with neurological and psychiatric disorder. This allows identifying which areas of the brain are functioning normally and which are under or over active. Functional magnetic resonance imaging, fMR shows instantaneous neural activity to see how the brain responds to specific stimulus. EEG, electroencephalogram can give the electrical activity in the brain in which brain cells communicate with each other through electrical impulses. Both PET and SPECT can detect brain function and blood flow. Brain PET study offers better image resolution than SPECT study but the acquisition takes time and can be uncomfortable and anxiety to patients with higher cost than SPECT imaging. SPECT imaging procedure is reliable and easy for scanning (2).

The American College of Radiology (ACR) published the guidelines for using brain SPECT in the clinical indications for evaluating patients in cerebrovascular disease, suspected dementia including early detection, differential diagnosis, and in the pre- dementia phase, epilepsy, pre-surgical localization of epileptic foci, traumatic brain injury, especially in the absence of computed tomography (CT) and/or magnetic resonance imaging (MRI) findings and assessing brain death (3).

The most commonly used radiopharmaceutical in regional cerebral blood flow (rCBF) SPECT is ^{99m}Tc labelling with hexamethylpropyleneamine oxime (^{99m}Tc HMPAO). To obtain the rCBF SPECT image, there is a need for using a radiopharmaceutical that reflects the rCBF. In order to represent the rCBF, the radiopharmaceutical needs to have the ability to pass the blood brain barrier (BBB) and thus be lipophilic. The radiopharmaceutical is further transported through the blood vessels and reaches the brain. The activity ratio of grey to white matter is approximately 2-3 to 1 which enables contrast and enhance tissue separation in the brain. On the other hand, there are still some limitations in brain SPECT imaging. The main weak point of brain SPECT imaging is that when the administered activity, scanning time or count rate is low, the image quality is poor and difficult for diagnosis. To compensate for this problem, the reconstruction parameters can be varied and optimized in order to improve the image quality in terms of contrast to noise ratio on brain SPECT images (4).

Image quality in nuclear medicine is determined by several methods such as contrast, resolution, noise. The contrast-to-noise ratio (CNR) of lesion to background is essential for the detection of lesions in cerebral SPECT. Image quality can be

affected by choice of collimator, radionuclide, and amount of administered activity, acquisition and reconstruction algorithm. One of the aims of nuclear medicine imaging research is to optimize the design of imaging systems and to improve qualitative and quantitative accuracy of reconstructed images. Optimization refers to the process of adapting the radiation dose as small as reasonably achievable, still ensuring that the needed diagnostic information is obtained (5). Proper image reconstruction depends on the ability to select appropriate reconstruction parameters which produce brain SPECT images that maximize the information from the acquired counts to obtain the greatest sensitivity and specificity for disease detection.

The goal of SPECT image reconstruction is to determine the three-dimensional distribution of radiopharmaceutical in the patient. The technique used to reconstruct the image is based on either analytical or iterative methods. The filtered back projection (FBP) algorithm is analytical reconstruction method. An iterative reconstruction method is generally used for image reconstruction of brain SPECT imaging although filtered back projection method is still used. Parameters of the iterative reconstruction, including the number of iterations and subsets, and the post-filtering substantially affect the image quality and might be determined by a phantom study that imitates the amount and distribution of radioactivity in the human brain SPECT imaging. Therefore, optimization of reconstruction parameter is required to obtain better image quality especially in low count SPECT imaging (6).

1.2 Research Objective

The aim of this study is to optimize the activity concentration and the reconstruction parameters on ordered-subset expectation maximization (OSEM) iterative reconstruction and filtered back projection (FBP) on $^{99m}\text{TcO}_4$ brain SPECT imaging based on Hoffman brain phantom study.

1.3 Definition

Single Photon Emission Computed Tomography (SPECT)

An imaging modality allows visualizing functional information of a patient's specific internal organ or body system using the distribution of radionuclide in the target organ in three dimensions (3D).

Computed Tomography

Computed Tomography is a technique for reconstructing three dimensional images of the structures at a particular depth within the body done by taking several x-ray images at different angles and then using computer software to reconstruct and analyze the resulting images.

Image Reconstruction

The projections acquired from many different angles around the body by one or more rotating detectors are then reconstructed and put together to form 3D images of the body. The reconstruction of tomographic images is made by two methods: filtered back projection and iterative methods.

Attenuation effect

Attenuation occurs when photons interact with matter and lose their energy. The processes of attenuation in nuclear medicine occur due to interaction in tissue at photon energies in the interval within 70 – 360 keV. Attenuation of photon means that the number of primary detected photons which have not interacted, decreases along their path through tissue or any sort of matter by absorption and scattering.

^{99m}Tc ECD (ethylene cysteine diethyl ester)

It is cerebral perfusion agents that is indicated for assessing regionally brain blood flow and diagnose functional changes in the case of Alzheimer's disease, investigation of epilepsy and dementia examinations.

Becquerel

The Becquerel is a unit of radioactivity corresponds to one disintegration per second (dps). (1 Curie= 3.7×10^{10} Bq, disintegration per second).

Activity concentration

The concentration of radioactivity within a given volume of tissue in absolute units. (Unit is mega Becquerel per cubic centimeter)

Regional cerebral blood flow in brain (rCBF)

The amount of blood flow to a specific region of the brain.

Image Noise

Image noise arises from the limited number of counts. It is a problem in SPECT imaging, which degrades the image quality by reducing the contrast. The image contrast is often measured as the signal to noise ratio and thus a high noise level implies reduced contrast.

Spatial Resolution

Spatial resolution refers to a SPECT camera as the ability to spatially resolve two sources of radioactivity at minimal distance as separate items.

CHAPTER II

REVIEW OF RELATED LITERATURE

2.1 Theory

2.1.1 Overview of brain perfusion SPECT

Brain perfusion SPECT is a functional neuroimaging technique that allows noninvasive study of physiologic and physio pathologic events in the human brain. With the appropriate technique and careful interpretation of the information provided, brain perfusion SPECT has proven potential for patient management. SPECT has clinical value in the diagnosis, therapeutic management, and follow-up of patients.

2.1.2 Clinical Application of Brain Perfusion SPECT

SPECT can be used to define a patient's pathologic status when neurologic or psychiatric symptoms cannot be explained by structural neuroimaging findings. SPECT is sensitive in detecting impairment of regional cerebral function when CT or MRI shows only nonspecific findings such as cerebral atrophy. Different perfusion patterns have been associated with different types of dementia. SPECT has an impact on therapeutic decisions by differentiating dementia of Alzheimer's type from depressive pseudo dementia, which can be effectively treated and presents with prefrontal perfusion impairment. Brain perfusion SPECT contributes to the knowledge of the pathophysiologic basis of neurologic and psychiatric diseases. The ability of SPECT to detect regional cerebral blood flow (rCBF) variations in different conditions has favored the investigation of sensorial, motor, and cognitive activities and the central effects of central nervous system (CNS) both the normal and the abnormal brain. In practice, visual evaluation of SPECT images alone is frequently limited in assessing subtle variations in regional tracer uptake, and quantification is thus required in clinical research (7).

2.1.3 Transport and behavior in human brain

To obtain an rCBF-SPECT image there is a need for using a radiopharmaceutical that reflects the rCBF. In order to represent the rCBF, the radiopharmaceutical needs to have the ability to pass the Blood Brain Barrier and thus be lipophilic. The lipophilic compound of radiopharmaceutical is following intravenous administration and is rapidly bound to protein. The radiopharmaceutical is transported through the blood vessels and reaches the brain. The extraction fraction, which describes the amount extracted from the blood vessels to the brain, is about 80% for HMPAO and a large proportion is due to first pass extraction, which means the extracted amount during the first passage through the brain. The method of rCBF SPECT is based on the fact that the distribution of the tracers is proportional to the rCBF. The activity ratio of grey to white matter is approximately 2-3 to 1 for HMPAO which enables contrast and hence tissue separation in the brain (8).

Technetium-99m-ECD (Ethylene-L, L-dicysteine diethylester) is a neutral, lipophilic technetium complex with high stability, owing to the N_2S_2 core, that can be

used even several hours after preparation. It can easily pass through the blood–brain barrier and is captured in the brain cells. Compared with ^{99m}Tc -HMPAO, ^{99m}Tc -ECD exhibits different pharmacokinetics in humans, thus a direct comparison of these two tracers cannot be made: the use of one or the other tracer may be preferable, depending on the clinical case.

2.2 Principle of brain SPECT imaging

Brain SPECT imaging is acquired in step and shoot scanning mode through the patient in supine position. Although imaging of the object in different projections can give some information about the depth of the structure, tomographic scanners make a precise assessment of the depth of the structure in an object.

2.3 Photon attenuation

Gamma ray photons are attenuated in body tissue while passing through a patient. The degree of attenuation depends on the photon energy, the thickness of the tissue and the linear attenuation coefficient of the photons in tissue. Techniques are employed to correct for attenuation. In one method, an uncorrected image is taken and the thickness of tissue through which the photons are attenuated of estimated. Using constant linear attenuation coefficient of the photons in tissue, each pixel data is correct to this equation to reconstruct the image.

$$I_t = I_0 e^{-\mu x}$$

If the photon beam initial intensity I_0 passes through an absorber of thickness x , then the transmitted beam I_t is given by exponential equation, where μ is the linear attenuation coefficient of absorbing for photon of interest and has a unit of cm^{-1} . The factor of $e^{-\mu x}$ represents the factor of the photon transmitted. Assumption of a constant linear attenuation coefficient can be useful for symmetric organs with similar tissue density, and it is not valid for several organs such as the heart, cause of the close proximity to other organs. Gamma ray traversing different thicknesses of various body tissues may be detected within the photo peak and therefore a constant correction factor may not be sufficient for attenuation correction. Attenuation corrections are not applied to SPECT images for reasons of complexity of the problem (8).

Attenuation correction can be made in different ways; common for them all is that they are based in finding out values for the actual mass attenuation coefficient by using transmission data. Today it is common to use hybrid systems where the SPECT camera is combined with a CT (computed tomography). By incorporating the techniques of CT in the image acquisition and reconstruction process it becomes possible to make a careful attenuation correction by using the detailed 3D density map that CT provides. The attenuation map is estimated by segmentation of anatomical structures and smoothing of voxel values to a size which is adapted for SPECT image voxel size, together with transformation of Hounsfield units to linear attenuation coefficients, μ , for the relevant photon energy. High quality and high spatial resolution images of cross sectional anatomy can also be provided within these hybrid systems, which gives the observer good anatomical landmarks that can be correlated to the SPECT image. Attenuation correction using CT data can be

incorporated in an iterative reconstruction method (9).

2.4 Scatter effect and correction

The primary mechanism for attenuation is Compton scattering, which results in changes in photon directions of travel with loss of energy may result in missed count thus reduced contrast together with higher noise level. One way to overcome or reduce the problem with scatter is to use a small energy window, so that only primary photons are detected. Scatter is a more significant problem at low photon energies because the percentage of scatter in the energy window is decreasing with increasing photon energy. During Compton scatter, the photon will deliver a part of its energy to the electron, and will continue with the remaining energy, scattered an angle θ . The energy of the scattered photon, $h\nu'$, can be calculated as:

$$h\nu' = h\nu \frac{1}{1 + \frac{h\nu}{m_0c^2} (1 - \cos \theta)}$$

Where m_0 is the rest mass of the electron and c is the speed of light. Different scatter correction methods are available and is often included in the reconstruction algorithm. The scatter can be estimated by using one or two additional energy windows, which are located next to the full absorption peak, and from them estimate the number of scattered photons in the primary energy window. A drawback with removing photons from the data is that the noise increase. When using window-based scatter correction methods in an iterative reconstruction is the scatter component added to the guessed image in the forward projection step. Because of adding photons instead of removing, it does not provide the same problem with noise (9).

2.5 SPECT/CT

The advantage of combining SPECT with CT is numerous and is primarily due to the anatomic referencing and the attenuation correction capabilities of CT. Combined SPECT/CT imaging provides sequentially functional information from SPECT and the anatomical information from CT, obtained during a single examination. CT data are also used for rapid and optimal attenuation correction of the single photon emission data and precise location of abnormal area and physiological tracer uptake. SPECT/CT improves sensitivity and specificity, but can also aid in achieving accurate dosimetry estimates as well as in guiding interventional procedure or in better defining the target volume for external beam radiation therapy. The development of instruments, computer-based procedures for image analysis and display, new radioisotope labelled agents for visualization of biologically significant events enhance the SPECT/CT in term of clinical impact on patients care and cost effectiveness. SPECT/CT data also provide a better region of interest for quantification of radiopharmaceutical uptake in a lesion. (10).

2.5.1 Data Acquisition

Data acquired by rotation the detector head around the long axis of the patient over 180 degrees, which minimizes the effects of attenuation. In the step and shoot mode, the detector moves around the patient at selected incremental angles and

collects the data for the projection at each angle. Other variable factors are the size of the pixel, the average number of counts collected in each pixel, and the number of views obtained. In general, the pixel size should be less than one-third the system resolution.

2.6 SPECT Reconstruction

Methods of image reconstruction using the acquired data fall into two categories: iterative methods and analytic methods. Analytic methods are based on exact mathematical solution to the image reconstruction problem, whereas iterative methods estimate the distribution through successive approximations. Accurate correction for attenuation and their degradations require more complex iterative reconstruction techniques. There are two main types of mathematical algorithms for image reconstruction; analytic reconstruction (filtered back projection) and iterative reconstruction (11).

2.6.1 Filtered back projection

The main steps involved in a filtered back projection image acquisition include:

- (1) Forward projection (data acquired and forward projected into sonogram space)
- (2) Data is filtered (the filter in filtered back projection)
- (3) Filtered sonograms are back projected into image space (the back project in filtered back projection).

Simple Back-projection is the earliest image reconstruction method. It is images from the raw data and takes the line data from the projection profiles, back-projection into a two-dimensional image. The major problem with the simple back-projection is that it leaves extra counts on the image in the wrong place causing star artifacts. Ramp filter is required to remove the blurring caused by the simple back-projection. The combination of back-projection and ramp filtering is known as filtered back projection. Ramp filter is a high-pass filter; it greatly amplifies the noise present in projection. The quality of images is degraded because of the presence of excessive noise in the reconstructed images.

2.6.2 Iterative Reconstruction

Iterative reconstruction technique requires many more calculations and much more computed time to create a trans-axial image than does FBP. It is a method of algorithms used to reconstruct 2D and 3D images from the projections of an object. There are several types of iterative reconstruction methods available, for example MLEM (Maximum Likelihood Expectation Maximization) and OSEM (Ordered Subsets Expectation Maximization). A fundamental difference between iterative and analytic image reconstruction methods is that the image is estimated in several steps through optimization in the iterative method, unlike the analytical method in which the calculation of the image matrix is made in a single step based on an analytical formula. (6).The iterative reconstruction methods have several advantages over the analytical methods. An iterative method can include corrections in the model for

example of non-homogeneous attenuation, scatter, and collimator blurring and septum penetration of high energy photons (12).

2.6.3 Image Filtering

In SPECT reconstruction, the brain images are filtered for manipulate processing to require for better visualization and quantization. Noise reduction is one of the important factors and which degrades the image quality. The problem of noise in SPECT was corrected with selected low pass filter. These filters were designed to suppress signals with high spatial frequencies. The image smoothing is determined by range of factors including the physical characteristic of tracers, the attenuation characteristics of region, and the preferences of the physician interpreting the scan. Image filtering was used to reduce the noise and preserve as much signal as possible. Characteristics of filters are described by two parameters.

2.6.4 SPECT Filtering

An image can be decomposed into summation of different spatial frequencies and the Fourier transforms converts an image into frequency space. The Fourier transform is a mathematical procedure which decomposes a signal into its sinusoid components with different frequencies. An inverse Fourier transform reconverts an image in frequency domain to spatial domain [8]. High frequency components of image response for simulating the rapid change intensity (edge and noise). Low frequency components of an image response for simulating amplitude of waveform. (contrast and intensity) (6).

2.6.5 Filter characteristics

Characteristics of filters are described by two parameters.

2.6.5.1 Cutoff frequency (f_c) or Critical frequency

It determines how much smoothing the filter applied by the filter. The lower cut-off frequency the smoother the image will look. Higher cut-off frequency gives noisier image. The units of cut-off frequency (f_c) vary considerably between SPECT systems suppliers. To understand and be able to relate frequencies from different manufacturers, Nyquist frequency is required. The Nyquist frequency is, by definition, 0.5 cycles per pixel and depends on pixel size of image matrix, which in turns depends on matrix size and the acquisition or reconstruction zoom factor.

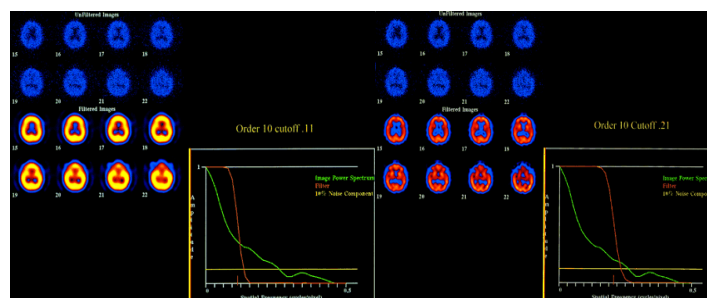


Figure 2.1 Effect of varying cut-off frequency of Butterworth filter (0.21 and 0.11) of order $n=10$.

2.6.5.2 Order

Order is a parameter that controls the slope of filter (Figure 2.2).

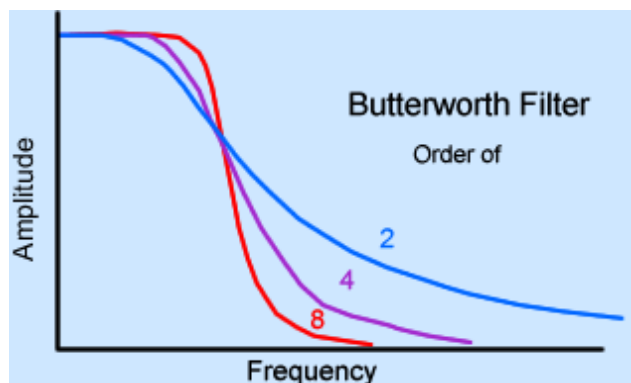


Figure 2.2 Same cut-off frequency and varying order

There are basically two types of filter used in SPECT, the smooth and enhancement filters. The former used low pass filter allowing the user to select the cut-off frequency. Other types of filter are resolution recovery.

1. *High Pass Filter*- This filter allows high frequency information pass and remove low frequency information.

2. *Low Pass Filter*-This filter- This allows low frequency information pass and reduces high frequency information. The examples of low pass filter are Hamming filter and Butterworth filter. The Butterworth filter is most popular low – pass filter. It has two parameters to define shape of this filter. The order controls the down slope and the cut-off frequency defines the width or spread of the filter.

2.7 Factors affecting image quality in brain SPECT

The image quality of nuclear medicine brain SPECT depends on many parameters including the nature of the radiopharmaceutical uptake (target to background ratio), acquisition time, patient motion, administered activity, total number of detected counts, scintillation camera, choice of collimator, reconstruction parameters of iteration and subsets, type of filter, attenuation correction etc. To achieve an optimized examination, each and every of these influencing parameters has to be optimized. Optimization of image quality in nuclear medicine is hence an extensive and time consuming work.

2.8 Review of related literature

Sofia K et .al (8) reported an article optimization of activity level in regional cerebral blood flow (rCBF) SPECT using the observer study visual grading regression. They review to assess the activity level needed to achieve satisfactory diagnostic information in rCBF SPECT image quality by using visual grading regression. This study comprised a material of 21 consecutive patients with dementia issue that have undergone an rCBF SPECT examination. An administered activity of ^{99m}Tc labelled HMPAO was injected to all patients in the study. From one single

examination, five studies corresponding to different activity levels (500, 625, 750, 875 and 1000MBq) were generated by using a gated acquisition. Iterative image reconstruction, OSEM, including corrections for attenuation, scatter and distance dependent resolution was used. Three experienced observer's specialists in nuclear medicine evaluated the images by rating their confidence about the fulfilment based on seven image quality criteria. The result showed that in table 1, there is a significant difference in perceived image quality between 500MBq and the reference activity, 1000MBq, in five of the seven image quality criteria. No statistical significant degradation was found between any other activity level than 500MBq and the reference activity (1000MBq). They described that the activity level could be reduced without losing too much diagnostic information.

Table 2.1 Results of the VGR analysis using 1000MBq as reference level of activity.

Criterion	p-value /estimate	p-value /estimate	p-value /estimate	p-value /estimate
	1000 MBq vs. 875 MBq	1000 MBq vs. 750 MBq	1000 MBq vs. 625 MBq	1000 MBq vs. 500 MBq
1	Not significant	Not significant	Not significant	Not significant
2	Not significant	Not significant	Not significant	0,009670 / -0,62476
3	Not significant	Not significant	Not significant	0,002054 / -0,91580
4	Not significant	Not significant	Not significant	0,001575 / -0,75629
5	Not significant	Not significant	Not significant	Not significant
6	Not significant	Not significant	Not significant	0,019504 / -0,55771
7	0,015475 / 0,59	Not significant	Not significant	0,029642 / -0,50412

Alzimami K et al.(2) reported an article of an evaluation of 3D OSEM, and a comparison with FBP in ^{99m}Tc SPECT images. They reviewed to compare 3D OSEM, with filtered back projection (FBP) with an optimized set of filter parameters, both with and without attenuation correction (AC). The SPECT images of a Jaszczak phantom filled with uniform ^{99m}Tc solution, and capillary line sources with ^{99m}Tc were acquired using a Siemens e-Cam Dual Head Gamma Camera. The OSEM reconstructions were halted after 1, 4, 8, 12 and 24 iterations using 2, 4, 8 and 16 subsets. Gaussian 3D post reconstruction filter was used. The linear attenuation coefficient was set to 0.15 cm^{-1} . The statistical significance of differences in contrast, noise and FWHM between different methods of reconstruction was assessed by a two-tailed T-test. Statistical significance was defined as $P = 0.01$. The results showed that, noise increases with increasing number of iterations. There is a significant increase in contrast with increasing number of subsets and iterations. In terms of noise, results have shown that 3D OSEM was significantly better than FBP for low count statistics and applying AC with 3D OSEM results in an improved image contrast in comparison to FBP as shown in figure 2.1. They concluded that the suitability of 3D OSEM for low count statistics studies compared to FBP, and the superiority of 3D OSEM with respect to FBP in terms of noise and spatial resolution. Furthermore, 3D OSEM with AC may improve detectability due to significant improvement in contrast.

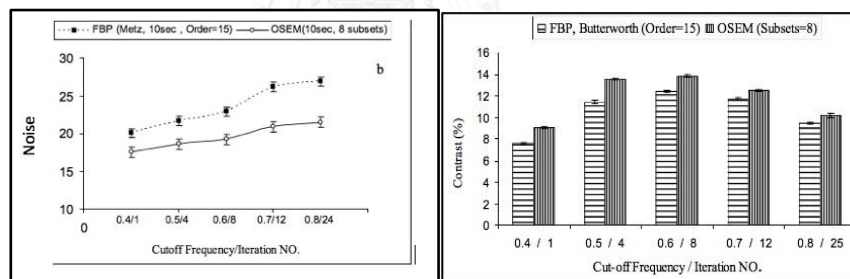


Figure 2.3 Relation between iteration no and cut-off frequency as function of % contrast and noise.

CHAPTER III

RESEARCH METHODOLOGY

3.1 Research design

This study is an experimental study. The steps of the procedure are shown as the following figure 3.1.

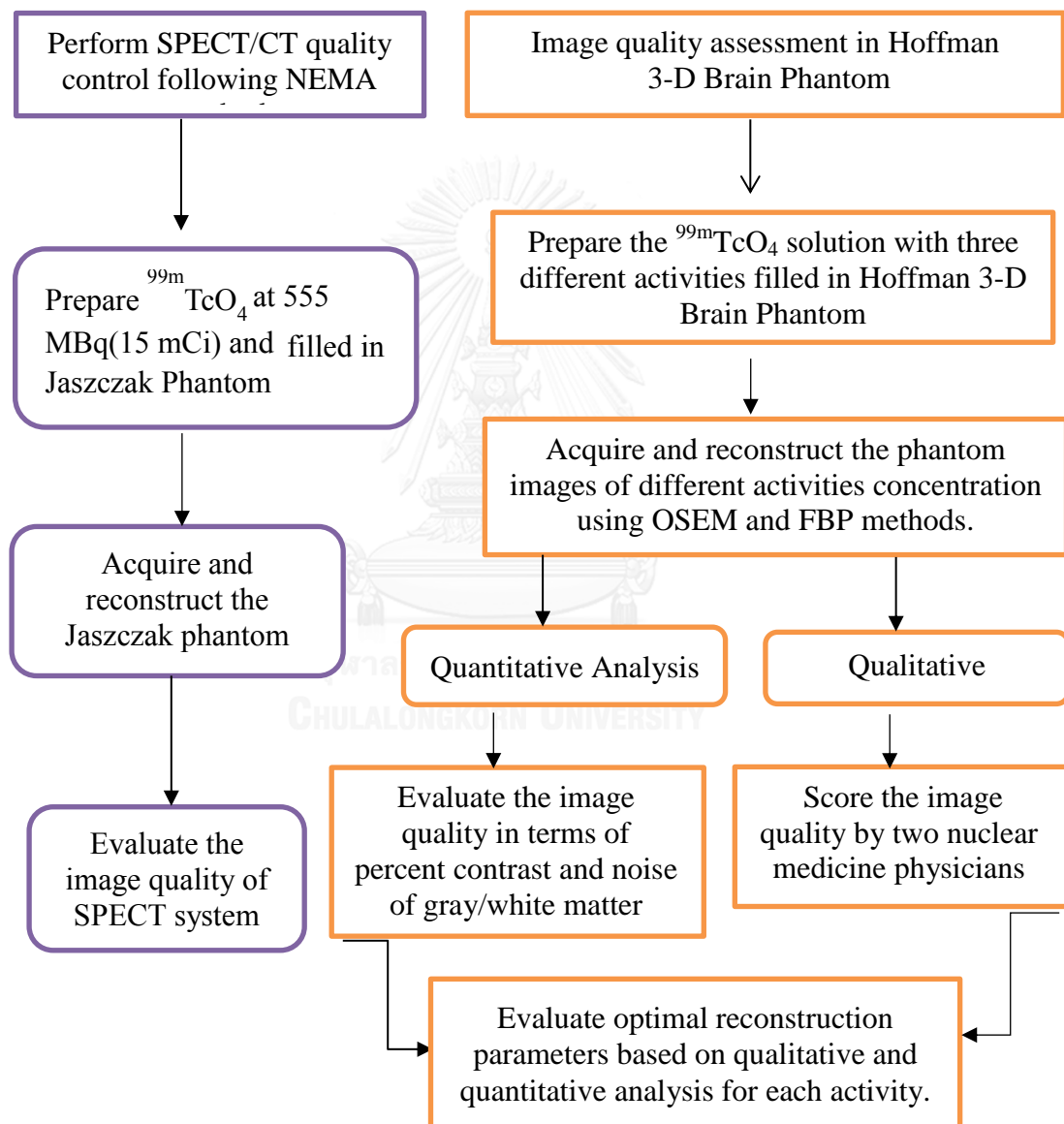


Figure 3.1 Research Design Model

3.2 Conceptual framework

Since the factors influencing the image quality of brain SPECT were OSEM and FBP reconstruction parameters, the conceptual framework of this study is shown as in figure 3.2.

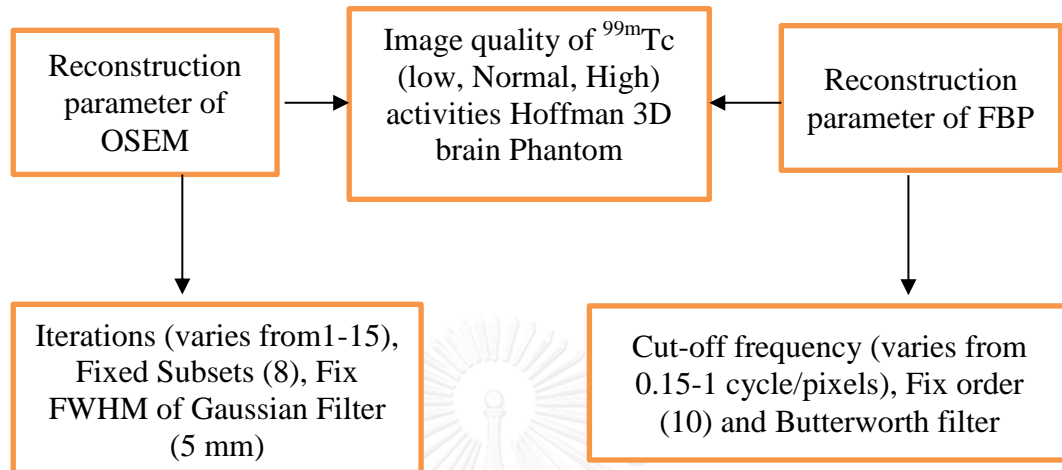


Figure 3.2 Conceptual framework

3.3 Research Question

What are the optimal reconstruction parameters of OSEM and FBP methods to accept the image quality in 3-D Hoffman Brain Phantom SPECT/CT at different activity?

3.4 Keywords

1. SPECT/CT
2. RECONSTRUCTION PARAMETERS
3. ORDERED SUBSET EXPECTATION MAXIMIZATION
4. FILTERED BACK PROJECTION
5. OPTIMIZATION

3.5 The sample

$$N = \frac{2(Z_{\alpha/2} + Z_{\beta})^2 \sigma^2}{MCD^2}$$

$$N = \frac{2(2.58 + 1.64)^2 (1.7)^2}{25}$$

$$N = 4.12$$

$$\alpha = 0.01$$

$$Z_{\alpha/2} = 2.58 \quad \beta = 0.1(90\%)$$

$$Z_{\beta} = 1.64$$

$$MCD = 5\% \text{ (Minimal Clinical Difference)}$$

$$\alpha = 1.7\% \text{ (from koyama et al 2008)}$$

The sample size of N is 4, but the activity concentration will vary three different activities of low, normal and high activity.

3.6 Materials

3.6.1 Single Photon Emission Computed Tomography/ Computed Tomography (SPECT/CT)

The SPECT/CT system model Symbia True Point T6 manufactured by Siemens Medical Solution as shown in figure 3.3 was installed in 2009 at Division of Nuclear Medicine, King Chulalongkorn Memorial Hospital, and Bangkok. The system integrates a SPECT scan with six-multi slice CT scans using Syngo multimodality computer platform. Dual SPECT detector of NaI (TI) crystal is 59.1x44.5 cm, field of view is 53.3x38.7 cm and the total number of photomultiplier tubes is 59. CT scan collects the data simultaneously via a 6- row detector. The maximum FOV is 50 cm, the gantry-bore diameter is 70 cm. Three kVp settings are available at 80, 110 and 130 kVp. The tube current ranges from 20 to 345 mA.



Figure 3.3 SPECT/CT System

3.6.2 Hoffman 3D Brain Phantom

The Hoffman 3D brain phantom as in figure 3.4 configured with simulation of the activity distribution in a flow or metabolic image of human brain. The phantom consists of “gray matter” and “white matter” fillable volume which is 1.2 liter. Cylinder inside diameter is 20.8 cm and inside height is 17.5 cm respectively. The phantom is comprised of sturdy plastic and a single fillable chamber that eliminates the necessity of preparing different concentrations of radioisotope. Nineteen independent plates stack neatly within the cylindrical phantom for easy disassembly and assembly (13)



Figure 3.4 Hoffman 3D brain phantom (left) and component of brain slabs inside the phantom (right).

3.6.3 Technetium pertechnetate ($^{99m}\text{TcO}_4^-$)

Technetium is obtained from a generator in normal saline solution (0.9% NaCl) as the pertechnetate ion, $^{99m}\text{TcO}_4^-$. Technetium-99m is a metastable nuclear isomer of technetium-99, symbolized as ^{99m}Tc . Technetium-99m is used as a radioactive tracer detected in the body. It is well suited to the role because it emits readily detectable 140 keV gamma rays and its half-life for gamma emission is 6.0058 hours. The short half-life of the isotope allows for scanning procedure, collect data rapidly but keep total patient radiation exposure low. In the brain SPECT scan, ^{99m}Tc -HMPAO or ECD is used. Scanning is performed with SPECT/CT. In a phantom study, $^{99m}\text{TcO}_4^-$ is used.

3.7 Methods

This study is carried out as the following.

3.7.1 SPECT/CT QC [APPENDIX A]

The quality control program for CT is performed using water phantom for the study of image quality, kVp calibration, pixel noise and CT number values. The quality control of SPECT/CT system was performed by following NEMA method. For SPECT system, the flood-field uniformity is evaluated intrinsically for the response of the detector operation. Uniformity is measured daily over the useful field of view and central field of view. The COR must be accurately aligned with the center of the acquisition matrix in the computer. The system image quality with JASZCZAK phantom, system planar sensitivity to test count rate response of scintillation camera.

3.7.2 The preparation of Hoffman 3D Brain Phantom

Three different activities of $^{99m}\text{TcO}_4$ solution were filled in the phantom with the activity of 55.5 MBq (1.5 mCi) for low activity acquisition, 111 MBq (3 mCi) for normal activity acquisition and 165.5 MBq (4.5 mCi) for high activity acquisition. The activity concentration of 46 kBq/cc, 92 kBq/cc and 138 kBq/cc were obtained for low, normal and high activity respectively. The administered activity of 15-20 mCi was used in routine clinical brain SPECT studies. The percent uptake to the brain is 5-7 percent. The normal activity of 111MBq (3 mCi) was calculated according to the clinical brain SPECT studies.

3.7.3 SPECT acquisition

SPECT acquisition was performed with a dual head gamma camera (Siemens Symbia True Point T6 SPECT/CT) and equipped with low-energy high resolution collimator (LEHR). The phantom was positioned in the center of field of view and perpendicular with X and Y plane of the detectors as shown in Figure 3.5. The image matrix size was 128x128 with a 2.7 mm pixel size and zoom factor was 1.78. The display FOV was 34.27 cm and was acquired with 180-degree circular step and shoot acquisition mode with 120 projections. The acquisition time was 30 minutes according to clinical brain SPECT protocol.

3.7.4 Reconstruction

For OSEM reconstruction, the number of subsets was fixed constantly at 8, the number of iterations was then varied from 1 to 15 (the range of OSEM updates 8-120) and then full width at half maximum (FWHM) of Gaussian filter was set at 5-mm. For FBP, the cutoff frequency for Butterworth filter was gradually changed from 0.15 to 1 cycles/pixel and the number of order was set as 10. Chang's attenuation correction was applied for both OSEM and FBP reconstruction methods (Table 3.1 and 3.2)



Figure 3.5 The Hoffman brain phantom acquired with SPECT/CT system

Table 3.1 Parameters for OSEM method

Reconstruction	Iteration number	Subsets (Fixed)	Iterative Updates	FWHM	Attenuation coefficient
OSEM	1-15	8	8-120	5-mm	0.12 cm^{-1}

Table 3.2 Parameters for FBP method

Reconstruction	Cut-off frequency	Order (Fixed)	Attenuation coefficient
FBP	0.15-1 cycles/pixel	10	0.14 cm^{-1}

3.7.5 Data analysis on image quality

The data were transferred to e-soft version Siemens software for data analysis. To investigate the basic properties of reconstruction parameters, gray/white matter percent contrast and noise were determined for each activity by manually contouring on the SPECT images of cerebellum, basal ganglia and vertex areas. All of these measured regions were under the agreement of nuclear medicine physicians for brain SPECT interpretation. In this study, 3D-OSEM and FBP reconstruction methods were characterized at different (low, normal and high) activity concentrations.

3.7.5.1 Quantitative analysis: Percent Contrast and Noise

Percent contrast can be calculated by using the average count per area (140 mm^2) in gray matter and white matter on basal ganglia, cerebellum and vertex of brain regions (fig 3.6) under the agreement of nuclear medicine physician. Percent contrast can be calculated by following this equation.

$$\text{Percent contrast} = \left[\frac{\text{GM Counts}/\text{mm}^2 - \text{WM Counts}/\text{mm}^2}{\text{GM Counts}/\text{mm}^2} \right] \times 100$$

Where GM and WM are ROI average counts on gray matter and white matter of phantom images. CT images were used for anatomical localization.

To get the consistency of ROI measurement used the same slice number, same area and same size of ROI of each activity measurement. The reason we have to calculate percent contrast for three regions is that when the physicians interpret the brain SPECT, they mainly focused on these areas. Figure (4.6) show three regions of brain area. Yellow circle represents the area of gray matter region and red one represents white matter region of the brain.

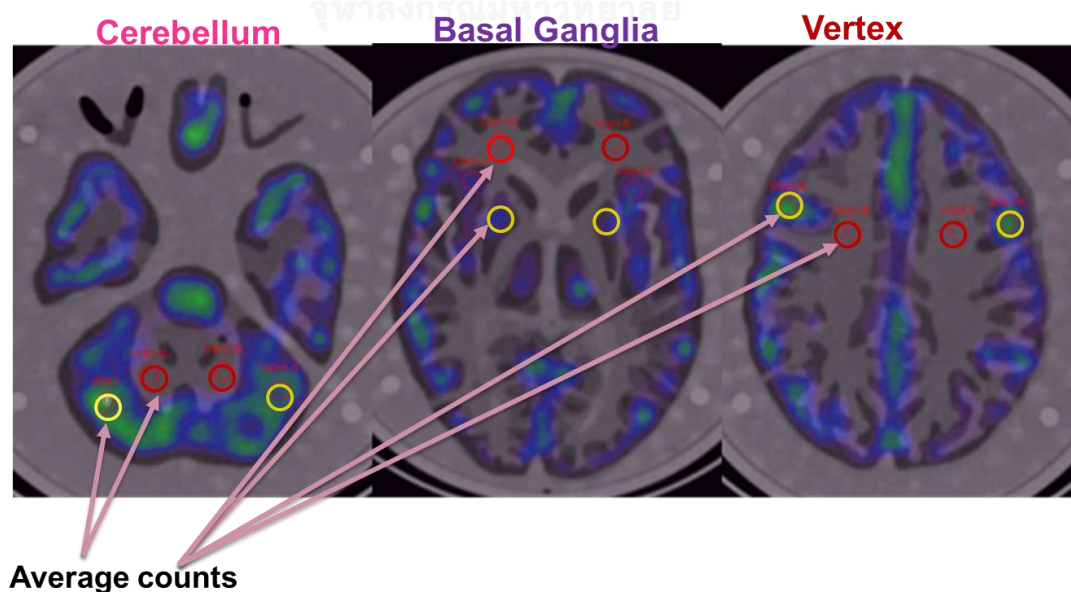


Figure 3.6 Percent contrast measurement on cerebellum, basal ganglia and vertex regions

Noise is linked with the standard deviation (SD) of the region of interest. Same ROI size of 140mm² was manually drawn on the gray matter of cerebellum, basal ganglia and vertex regions as same area of GM region shown in fig 3.6. For noise evaluation was drawn on the GM region of the brain because the activity is filled only in the gray matter region.

3.7.5.2 Qualitative Image Scoring

Image quality criteria scoring were determined by using seven image criteria (Table 2) of which five considered specific anatomic structures and the other two considered image quality in general according to image criteria scoring of Brain SPECT study from [Lund University, Sweden in 2012 at Department of Medical Radiation Physics](#) (8). The image quality criteria scoring were assessed by two experience nuclear medicine physicians by blinded observation. The image criteria are defined in Table.3.3

Table 3.3 Image Quality Criteria

IMAGE QUALITY CRITERIA	SCORE
1. "Grey and white matter are discernible in the cerebellum"	
2. "Grey and white matter are discernible in the medial and lateral parts of the temporal lobe"	
3. "Grey and white matter are discernible laterally in the frontal lobes"	
4. "Thalamus is bilaterally discernible"	
5. "White matter is discernible from the ventricles in the parietal lobes"	
6. "The noise level does not have a disturbing effect on the assessment"	
7. "Overall image quality is good enough to provide clinical diagnosis"	
Total Score	

Rate of image score

0 = completely certain that the criterion is not fulfilled

1 = almost that the criterion is partly fulfilled

2 = completely certain that the criterion is fulfilled

Acceptable of image quality score; total score ≥ 10 points.

3.8 Statistical analysis

Data from phantom study had been reported as maximum, minimum, mean and SD of counts on different activities by using excel program. Cohen's Kappa and ICC for inter-observer reliability was used to evaluate qualitative image quality analysis.

3.9 Data analysis

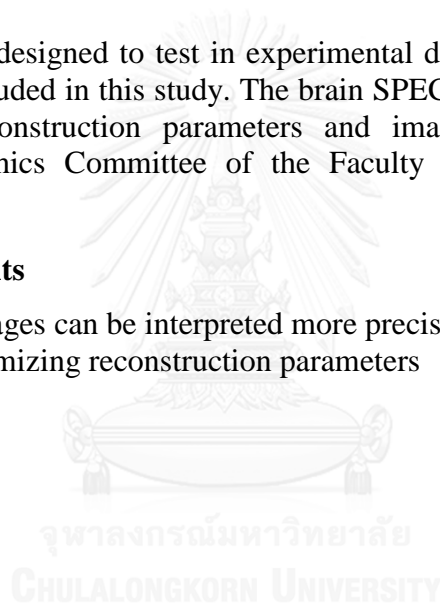
The quantitative image quality was analyzed by percent contrast and noise for each activity of phantom study as presented in form of table and bar graph. The qualitative image quality, using image scoring was analyzed by two nuclear physicians as presented in form of table and bar chart.

3.10 Ethical Consideration

This study is designed to test in experimental descriptive study. Hoffman 3D brain phantom is included in this study. The brain SPECT images are used in order to achieve optimal reconstruction parameters and image quality. This study was approved by the Ethics Committee of the Faculty of Medicine, Chulalongkorn University.

3.11 Expected benefits

The brain images can be interpreted more precisely especially in low activity concentration by optimizing reconstruction parameters



CHAPTER IV

RESULTS

4.1 Quantitative results in OSEM reconstruction

Table 4.1-4.6 show the percent contrast and noise of each activity concentration of various number of iteration from 1 to 15 at the cerebellum, basal ganglia and vertex area of each activity. The percent contrast was increased when the iteration number was increased from 1 to 15. On the other hand, noise in each region was represented by the standard deviation in the ROI of reconstructed images. The noise increased when the iteration number was increasing. In this study, the iteration number was varied from 1 to 15, whereas the subsets were fixed at 8, FWHM of Gaussian post reconstruction filter was fixed at 5mm and Chang's attenuation correction was applied at 0.12cm^{-1} for all activities

Table 4.1 Percent contrast vs number of iteration from 1-15 of low activity concentration

Percent contrast evaluation			
Iterations	Cerebellum	Basal ganglia	Vertex
1	45.71	52.78	50.23
2	47.83	54.67	52.69
3	50.53	56.41	55.26
4	54.05	60.00	58.97
5	56.76	61.63	60.98
6	57.89	62.76	61.91
7	59.79	65.11	64.09
8	61.19	66.31	66.67
9	62.79	67.92	67.75
10	62.96	69.15	68.09
11	63.68	71.37	69.39
12	64.68	71.70	70.91
13	64.44	72.12	70.92
14	65.06	72.73	71.09
15	65.27	73.21	71.09

Table 4.2 Noise vs number of iteration from 1-15 in GM region of low activity concentration

Noise Evaluation			
Iterations	Cerebellum	Basal ganglia	Vertex
1	6.00	7.9	7.30
2	7.10	8.5	8.16
3	7.90	9.6	9.00
4	9.00	11	10.14
5	9.60	11.9	11.13
6	10.80	12.6	11.98
7	11.60	13.6	12.79
8	12.00	14.00	13.43
9	12.70	15.00	14.30
10	13.90	16.00	15.40
11	14.40	17.00	16.13
12	15.20	18.20	17.40
13	16.50	19.00	18.70
14	17.00	20.30	19.00
15	18.00	21.00	20.00

Table 4.3 Percent contrast vs number of iteration from 1-15 of normal activity concentration

Percent contrast evaluation			
Iterations	Cerebellum	Basal ganglia	Vertex
1	52.50	61.00	61.37
2	57.57	64.68	63.52
3	60.12	68.86	67.24
4	64.79	70.97	71.34
5	66.71	73.03	72.23
6	67.11	74.26	73.85
7	69.64	74.49	74.62
8	70.04	76.39	75.71
9	71.19	78.38	78.08
10	72.13	78.74	78.37
11	74.64	80.95	78.66
12	74.60	81.25	79.61
13	74.98	81.71	80.20
14	75.00	81.71	80.25
15	74.38	82.35	79.61

Table 4.4 Noise vs number of iteration from 1-15 in GM region of normal activity concentration

Noise Evaluation			
Iterations	Cerebellum	Basal ganglia	Vertex
1	4.60	6.00	5.80
2	5.60	7.20	6.60
3	7.00	8.40	7.90
4	7.60	9.50	8.70
5	8.50	10.70	9.45
6	9.30	11.45	10.50
7	10.20	12.30	11.40
8	11.30	13.00	12.20
9	12.15	14.00	13.50
10	13.00	14.60	14.00
11	13.60	15.70	15.10
12	14.50	16.40	15.80
13	15.00	17.00	16.40
14	15.40	17.80	16.80
15	16.30	18.50	17.70

Table 4.5 Percent contrast vs number of iteration from 1-15 of high activity concentration

Percent contrast evaluation			
Iterations	Cerebellum	Basal ganglia	Vertex
1	60.42	66.07	65.06
2	63.46	68.33	67.62
3	65.72	69.84	68.83
4	68.45	72.47	71.55
5	69.49	75.22	73.85
6	70.45	76.81	75.37
7	72.13	77.75	76.97
8	73.54	78.93	77.78
9	75.85	81.01	79.45
10	77.55	81.88	80.51
11	77.97	82.93	81.01
12	78.23	83.93	84.19
13	79.28	83.95	82.72
14	79.41	84.52	82.93
15	79.78	84.88	83.52

Table 4.6 Noise vs number of iteration from 1-15 in GM region of high activity concentration

Noise Evaluation			
Iterations	Cerebellum	Basal ganglia	Vertex
1	3.21	4.90	4.30
2	3.90	5.30	4.90
3	4.60	6.00	5.30
4	5.70	7.00	6.50
5	6.60	8.40	7.80
6	7.30	9.40	8.80
7	8.00	10.30	9.60
8	8.70	12.00	11.34
9	9.40	12.70	12.01
10	10.70	13.80	13.00
11	11.80	14.00	14.21
12	12.60	14.30	14.81
13	13.00	15.80	15.40
14	13.50	16.70	16.00
15	14.00	17.60	16.71

Figures (4.1A, 4.2A and 4.3A) represent the relation between percent contrast and iterations number of the cerebellum, basal ganglia and vertex area of each activity. The noise increased when the iteration number was increasing as shown in figures (4.1B, 4.2B and 4.3B)

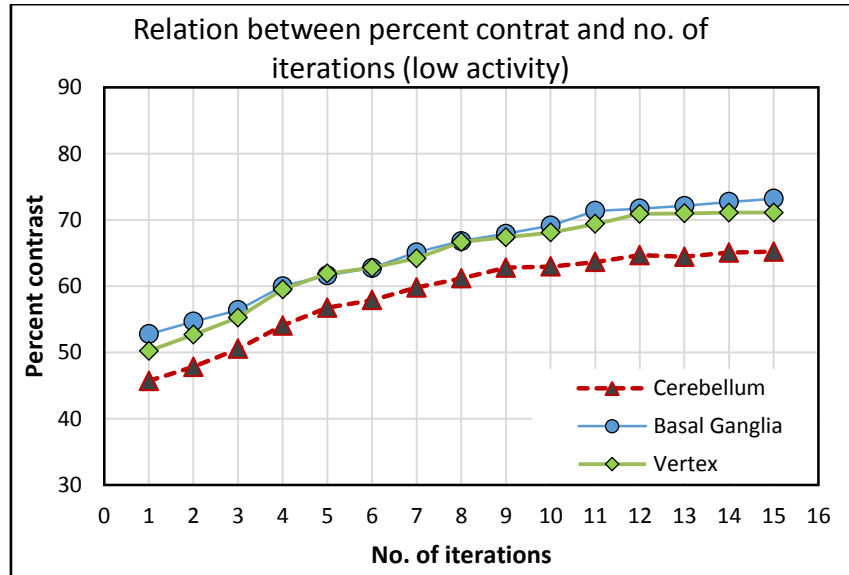


Figure 4.1A Relation between number of iterations and related percent contrast in low activity brain image

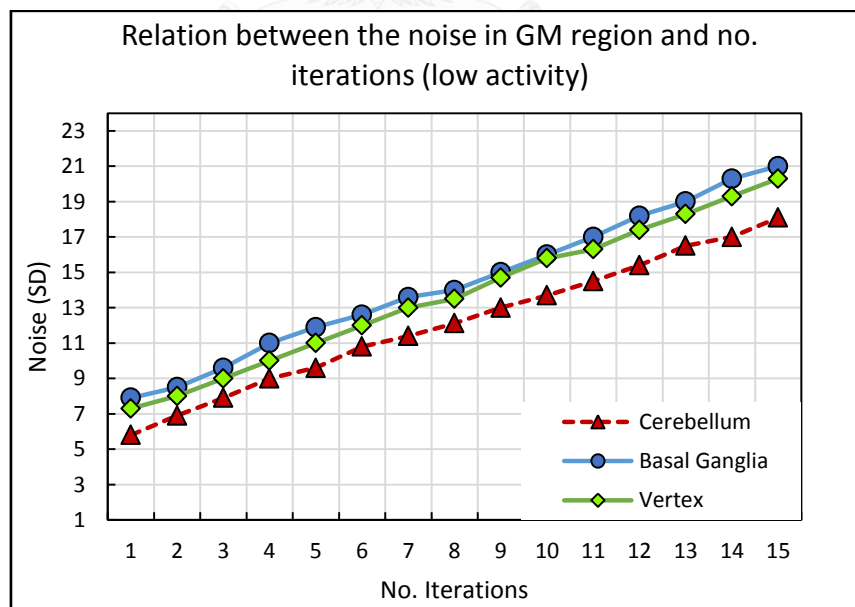


Figure 4.1B Relation between number of iterations and noise in low activity brain image

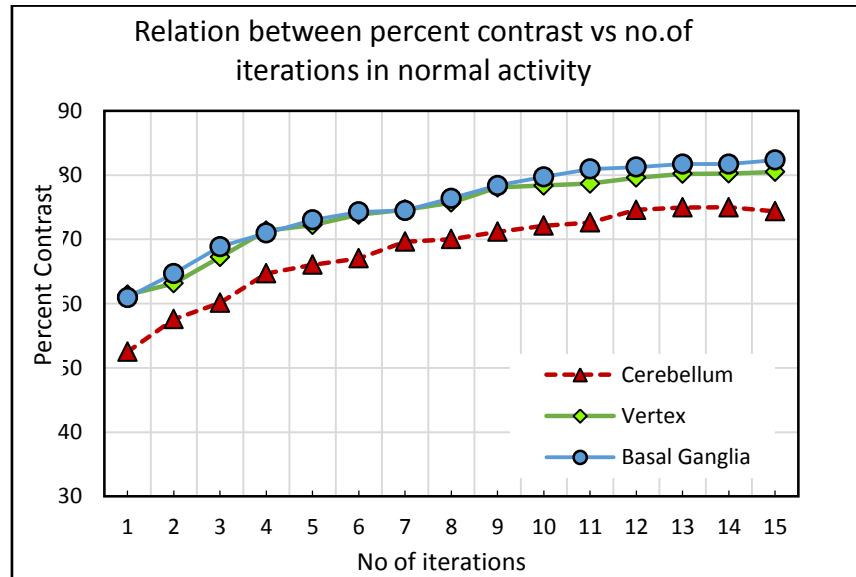


Figure 4.2A Relation between iterations number and related percent contrast in normal activity brain image

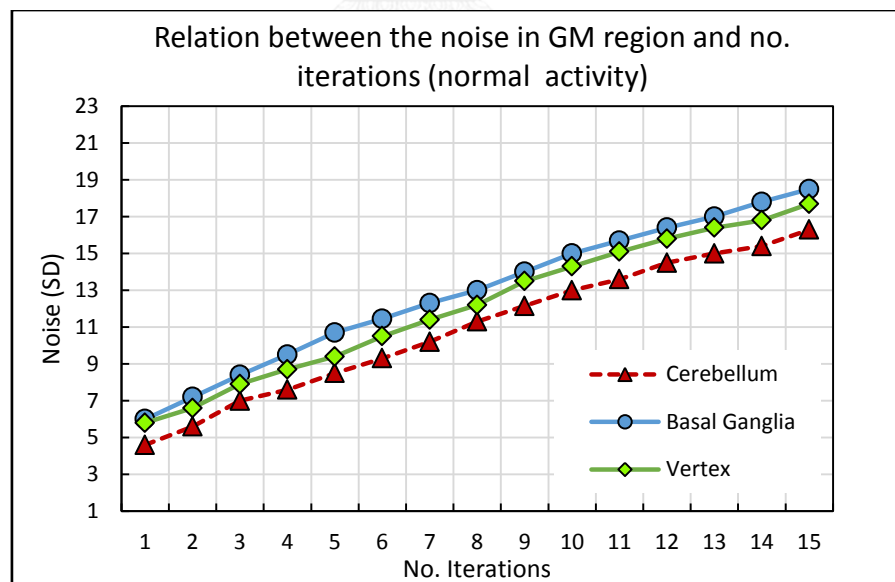


Figure 4.2B Relation between number of iterations and noise in normal activity brain image

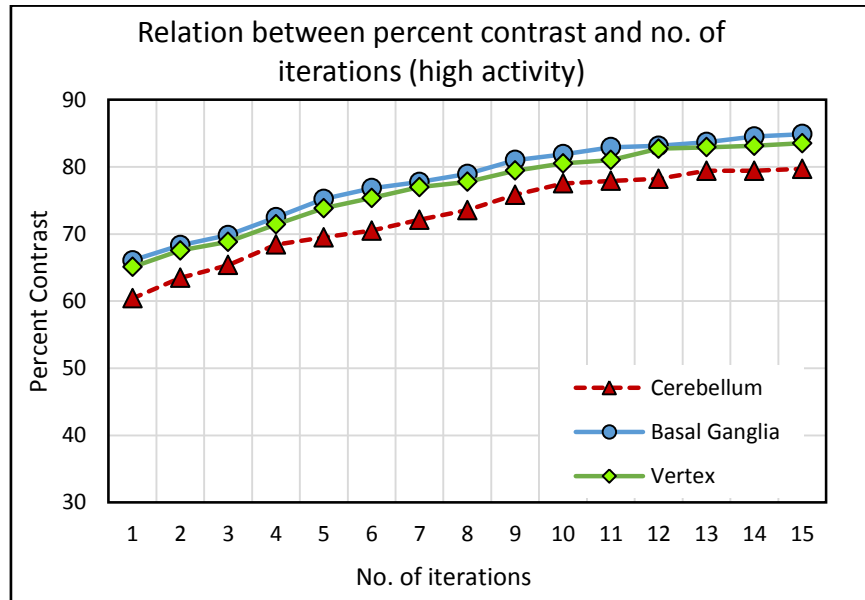


Figure 4.3A Relation between number of iterations and related percent contrast in high activity brain image

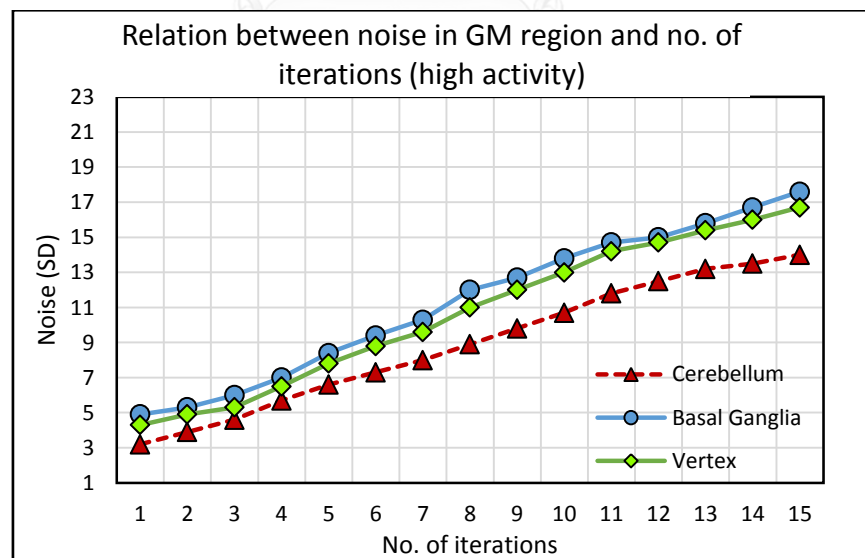


Figure 4.3B Relation between number of iterations and noise in high activity brain image

4.2 Quantitative results in FBP reconstruction

In FBP reconstruction, the cut-off frequency was varied from 0.15 to 1 cycles/pixel and the order value was fixed at 10 and Butterworth filter was applied Table 4.7 - 4.12 Percent contrast and noise of each activity based on the FBP reconstruction in varying cut-off frequency from 0.15-1 cycles/pixel.

Table 4.7 Percent contrast vs cut-off frequency for low activity concentration

Percent contrast evaluation			
Cut-off frequency	Cerebellum	Basal Ganglia	Vertex
0.15	40.11	45.45	45.16
0.25	42.28	49.43	48.13
0.35	46.22	52.78	50.15
0.45	49.14	54.21	52.98
0.55	50.24	55.76	54.73
0.65	51.00	57.23	55.11
0.75	51.68	57.50	56.27
0.85	52.40	58.54	57.45
0.95	53.80	59.26	57.58
1	54.28	59.36	58.18

Table 4.8 Noise vs cut-off frequency for low activity concentration

Noise evaluation			
Cut-off frequency	Cerebellum	Basal ganglia	Vertex
0.15	8.00	10.45	10.00
0.25	9.10	11.20	10.80
0.35	10.00	11.80	11.60
0.45	12.00	13.00	13.00
0.55	13.40	14.65	14.30
0.65	14.80	15.76	16.00
0.75	16.40	17.85	17.20
0.85	17.80	19.30	19.00
0.95	19.80	21.67	20.30
1.00	21.00	23.50	22.90

Table 4.9 Percent contrast vs cut-off frequency for normal activity concentration

Percent contrast evaluation			
Cut-off frequency	Cerebellum	Basal ganglia	Vertex
0.15	46.27	52.00	51.01
0.25	49.30	54.36	53.44
0.35	52.60	60.04	58.20
0.45	55.64	62.28	61.11
0.55	57.21	64.58	62.64
0.65	59.52	65.74	64.51
0.75	60.59	67.58	65.47
0.85	61.22	68.32	66.19
0.95	62.08	68.58	67.14
1	62.53	68.98	67.01

Table 4.10 Noise vs cut-off frequency for normal activity concentration

Noise evaluation			
Cut-off frequency	Cerebellum	Basal ganglia	Vertex
0.15	7.00	9.00	8.00
0.25	7.80	10.00	9.10
0.35	9.30	10.30	10.82
0.45	10.00	11.00	11.40
0.55	11.84	13.20	13.00
0.65	14.00	16.00	15.30
0.75	15.60	18.00	17.00
0.85	17.00	19.00	18.50
0.95	17.80	21.00	20.20
1	18.40	22.00	21.00

Tale 4.11 Percent contrast vs cut-off frequency for high activity concentration

Percent contrast evaluation			
Cut-off frequency	Cerebellum	Basal ganglia	Vertex
0.15	53.85	58.86	58.62
0.25	56.63	61.20	60.43
0.35	59.30	65.25	63.50
0.45	64.37	68.17	68.27
0.55	64.90	70.80	69.87
0.65	65.97	71.74	70.42
0.75	66.70	72.41	71.03
0.85	67.27	72.50	71.79
0.95	67.64	73.25	72.41
1	68.50	73.69	72.80

Table 4.12 Noise vs cut-off frequency for high activity concentration

Noise evaluation			
Cut-off frequency	Cerebellum	Basal ganglia	Vertex
0.15	6.70	8.30	7.70
0.25	7.30	9.00	8.40
0.35	8.00	9.70	9.20
0.45	8.90	10.70	10.10
0.55	9.80	11.40	11.00
0.65	10.90	13.00	12.00
0.75	11.80	14.00	13.30
0.85	12.80	15.20	14.20
0.95	14.00	16.40	15.60
1	14.50	17.20	17.00

Percent contrast was increased with an increasing the cut-off frequency from 0.15 to 1 cycles/pixel as shown in Figure (4.4A, 4.5A and 4.6A). For noise evaluation, noise showed continuously increasing when the cut-off frequency of 0.15 to 1 cycles/pixel was increased as shown in Figure (4.4B, 4.5B and 4.6B)

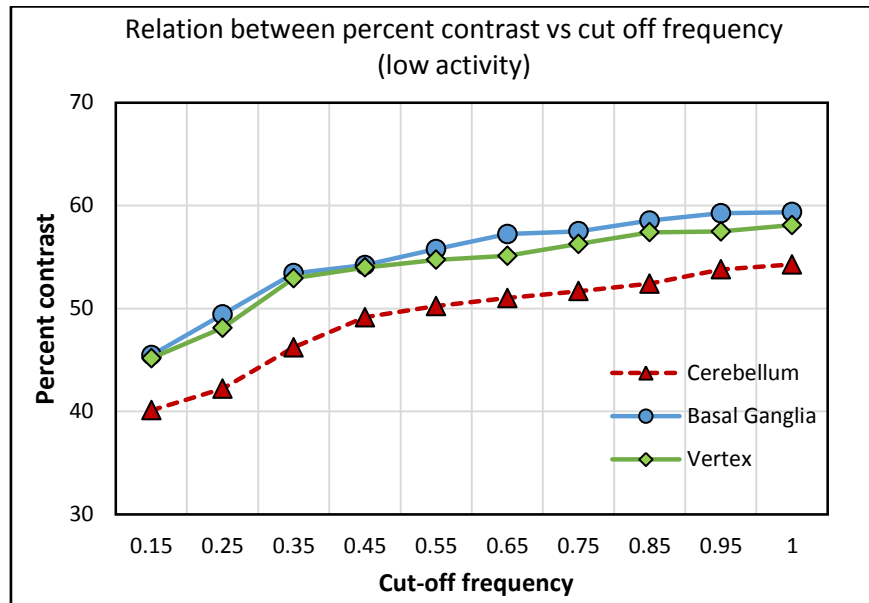


Figure 4.4A Relation between cut-off frequency and related percent contrast in low activity

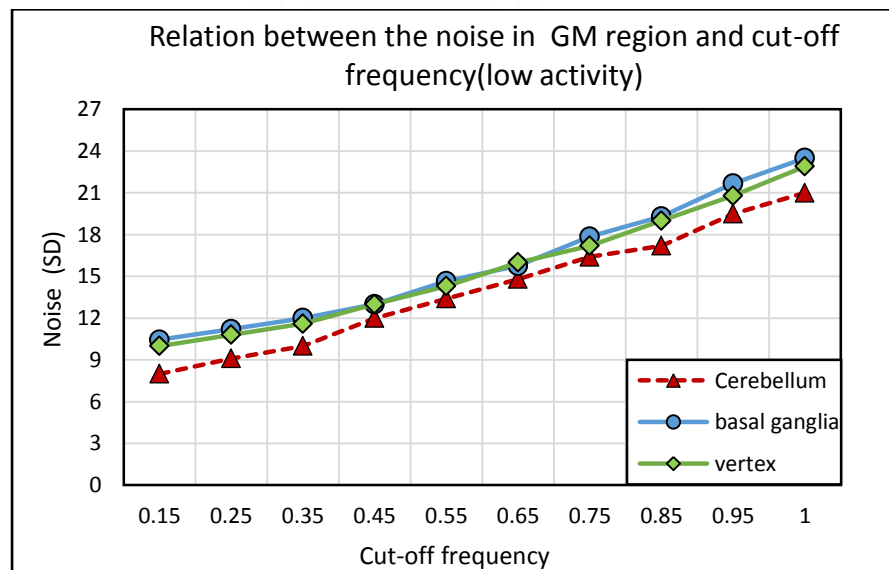


Figure 4.4B Relation between cut-off frequency and noise in low activity

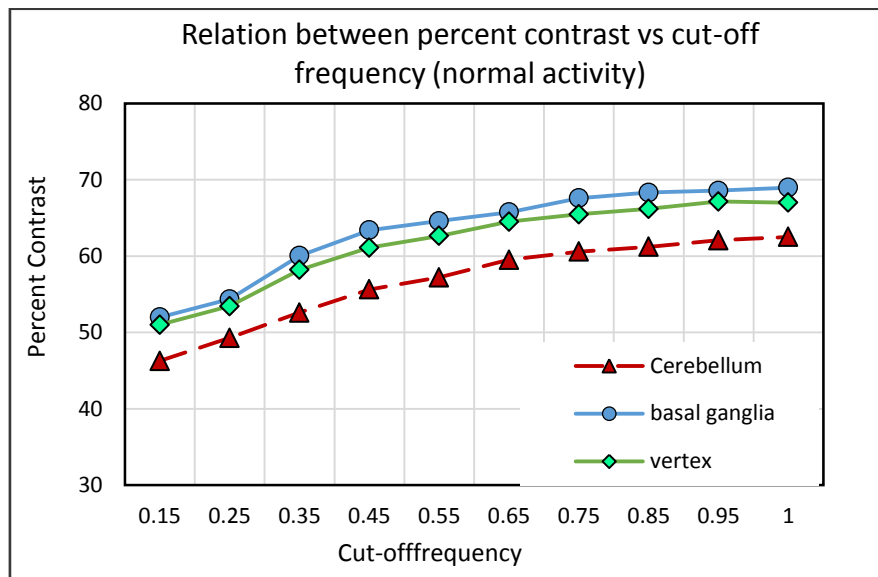


Figure 4.5A Relation between cut-off frequency and related percent contrast in normal activity

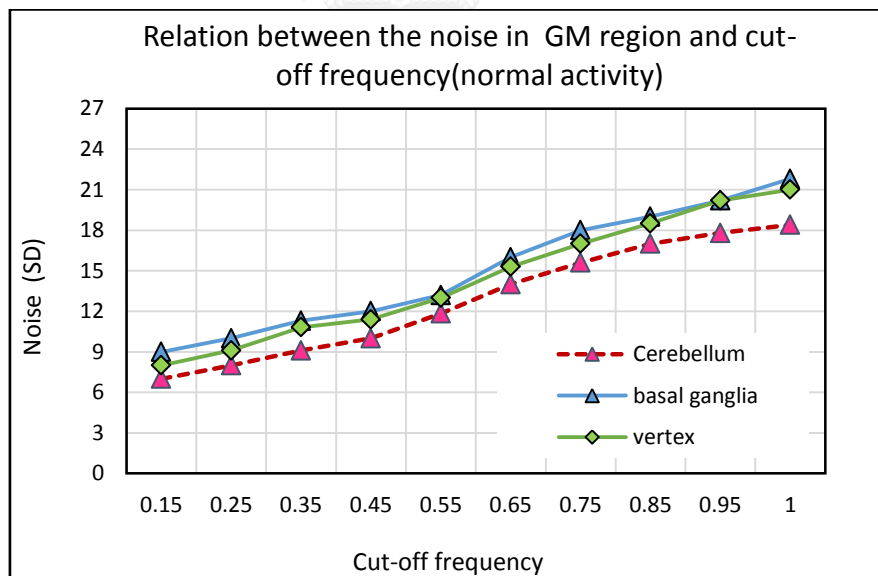


Figure 4.5B Relation between cut-off frequency and noise in normal activity

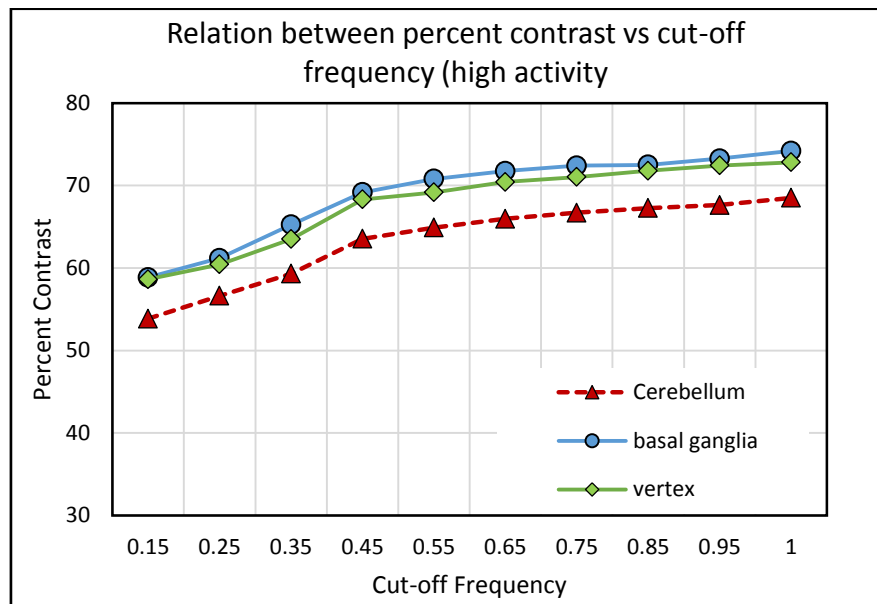


Figure 4.6A Relation between cut-off frequency and related percent contrast in high activity

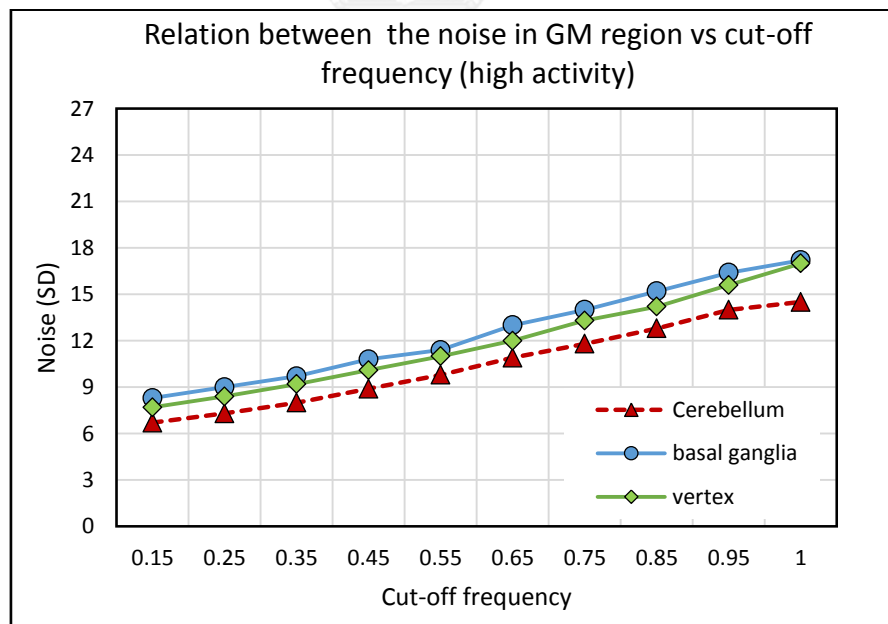


Figure 4.6B Relation between cut-off frequency and noise in high activity

Figure 4.7 and 4.8 show the brain SPECT images according to the varying parameters of each activity concentration. When the iterations number and cut-off frequency was increased, the image becomes sharper and can see detail inside the brain. But noise also increased with increasing iteration and cut-off frequency.

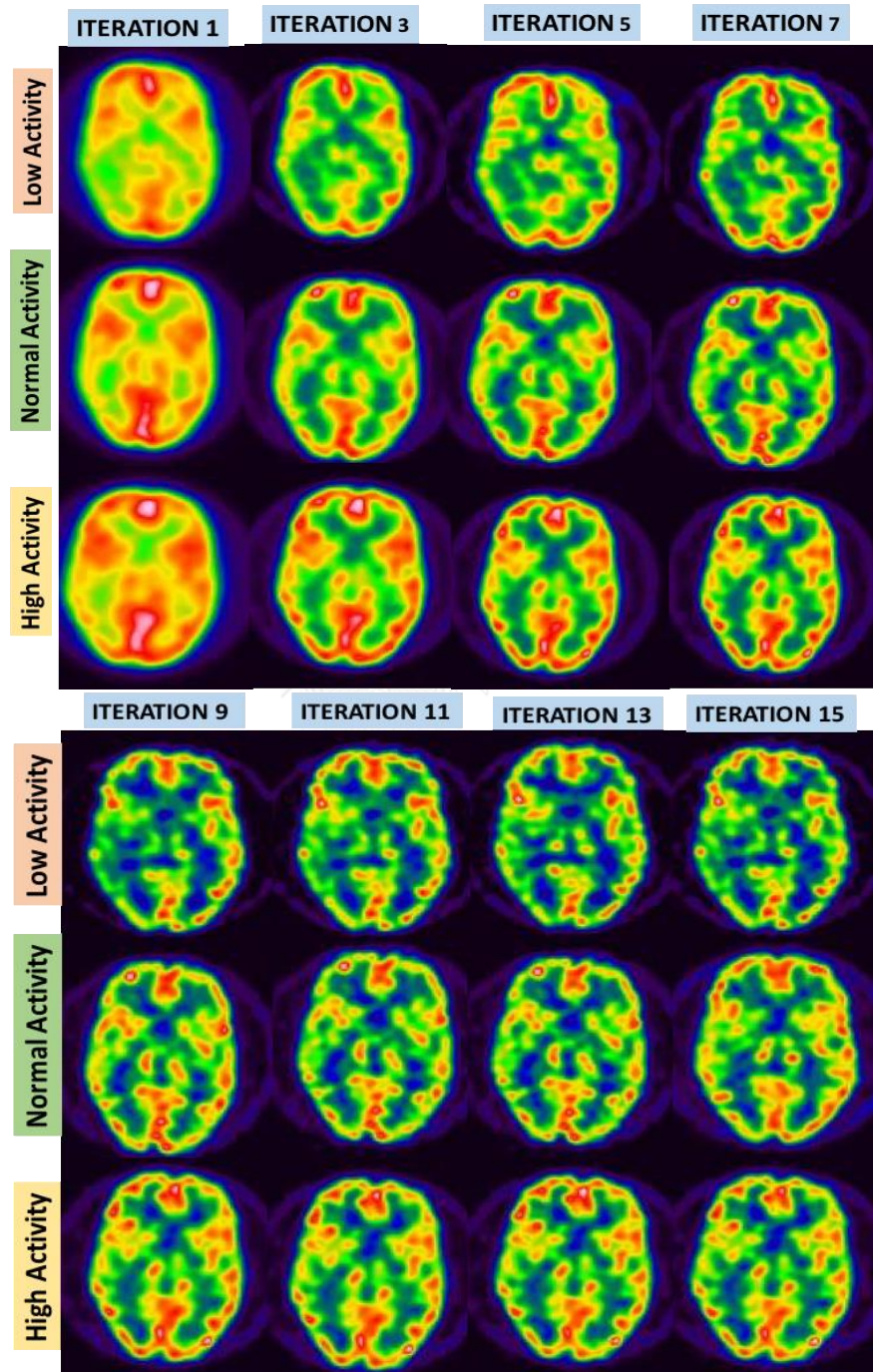


Figure 4.7 Brain SPECT images by varying number of iterations of 3 activity concentration in OSEM method

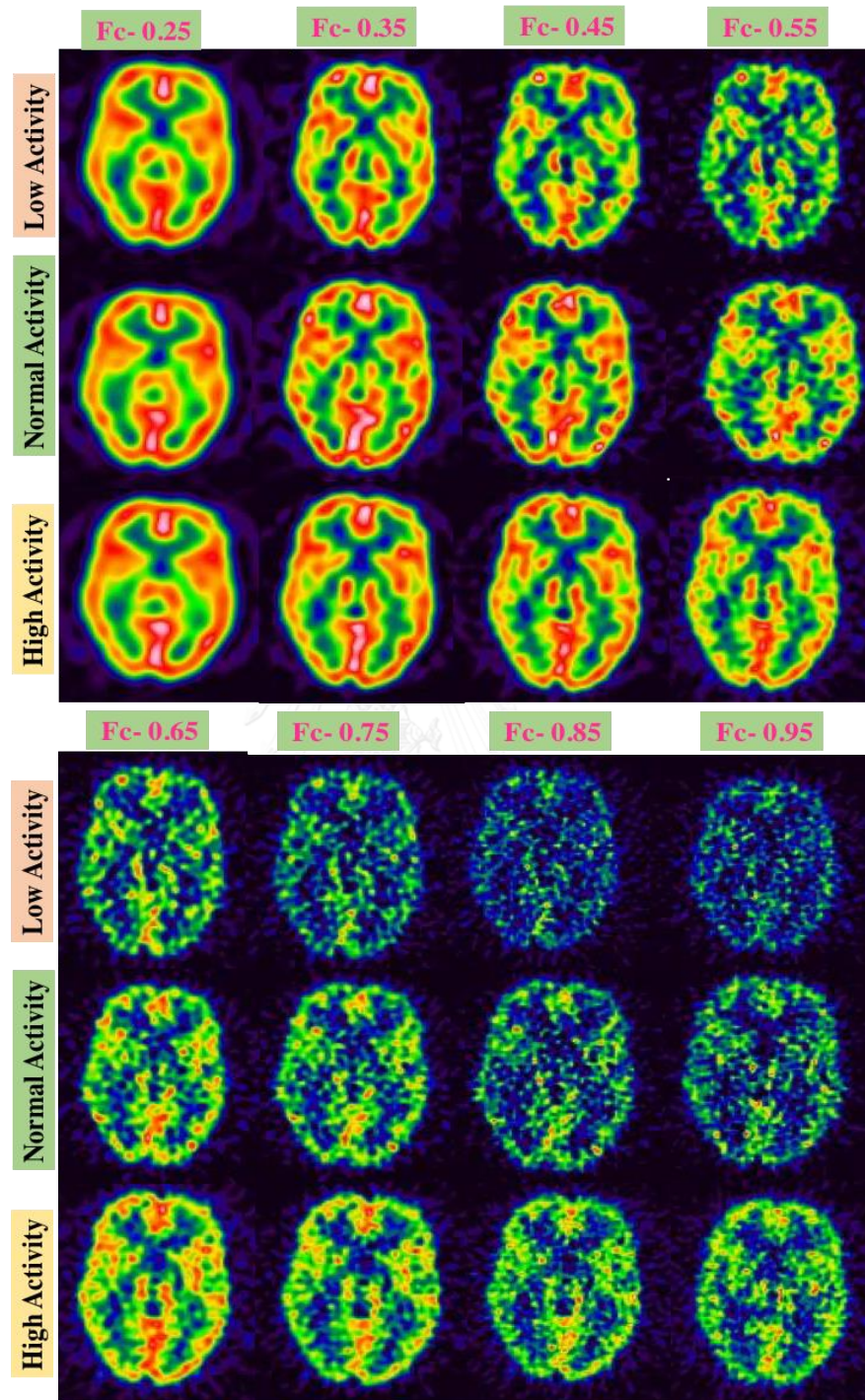


Figure 4.8 Brain SPECT images by varying cut-off frequencies of each activity concentration in FBP method

4.3 Qualitative Image quality evaluation, Scoring

Qualitative image quality was evaluated by two nuclear medicine physicians at Division of Nuclear Medicine, Faculty of Medicine, Chulalongkorn University and King Chulalongkorn Memorial Hospital. The experience of physician's observer 1 is over ten years working experience and observer 2 is over three years working experience respectively. The rate of image scores was (0 – 2) among seven image criteria as described in the chapter 3. Acceptable image score was ≥ 10 points of total score. Five image criteria were considered specifically in anatomical structures and the other two criteria were considered image quality in general.

ICC inter correlation coefficient) for the interpretation agreement between two nuclear medicine physicians of 0.58 was obtained for OSEM reconstruction and 0.40 for FBP image reconstruction. The calculation was done by using Microsoft excel as shown in table 4.13. The results of ICC referred to the strength of agreement between two readers. As a result, 0.58 and 0.40 were the values obtained from this study, which means the strength of agreement between two observers is moderate. (below 0.20 regarded as poor, 0.21–0.40 as fair, 0.41–0.60 as moderate, 0.61–0.80 as good and >0.80 as very good agreement) (14). For each criterion, the raters' scoring of Cohen's kappa k- value was within 0.65 – 0.4 which means good agreement between two raters.

Table 4.13 The strength of agreement between two observers by using ICC

	OSEM	FBP
Match	26	12
Total	45	30
ICC	0.58	0.4

Figure (4.9-4.11) shows the scatter plot of image quality scoring from two observers in OSEM reconstruction method. The scoring above the dotted line (≥ 10) was identified as acceptable scoring points.

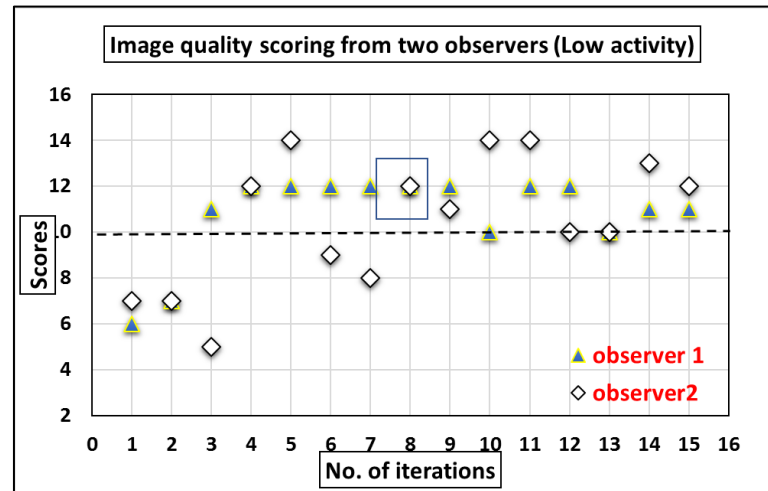


Figure 4.9 Scatter plot of image quality scoring Vs no. of iterations (low activity)

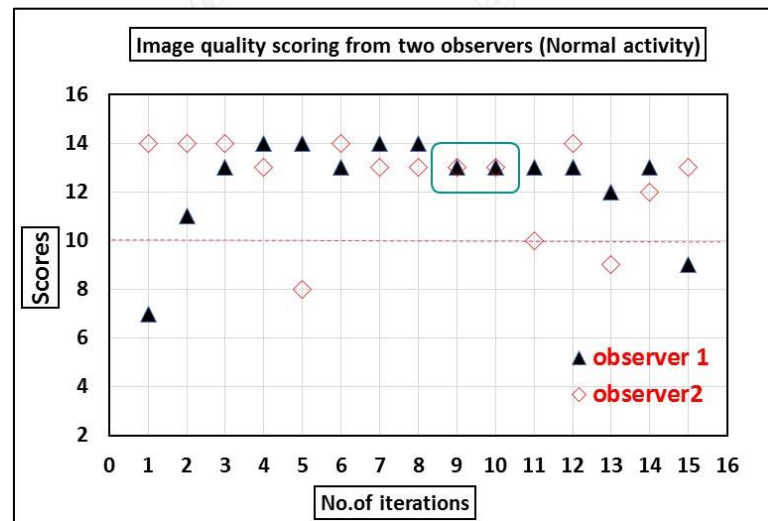


Figure 4.10 Scatter plot of image quality scoring Vs no. of iterations (normal activity)

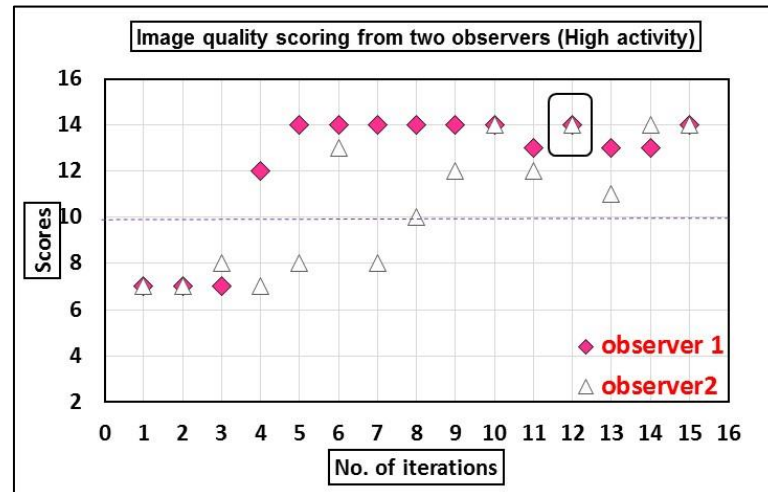


Figure 4.11 Scatter plot of image quality scoring Vs no. of iterations (high activity)

Figure (4.12 - 4.14) shows the scatter plot of image quality scoring from two observers in FBP reconstruction method.

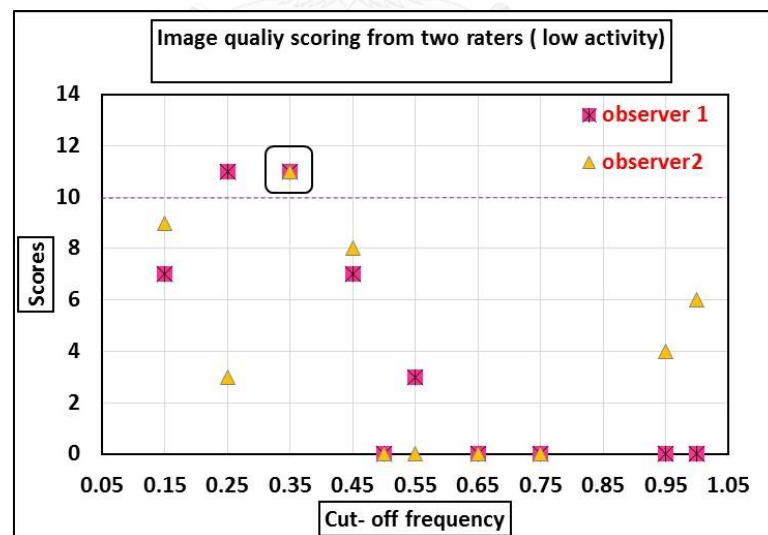


Figure 4.12 Scatter plot of image quality scoring Vs cut-off frequency (low activity)

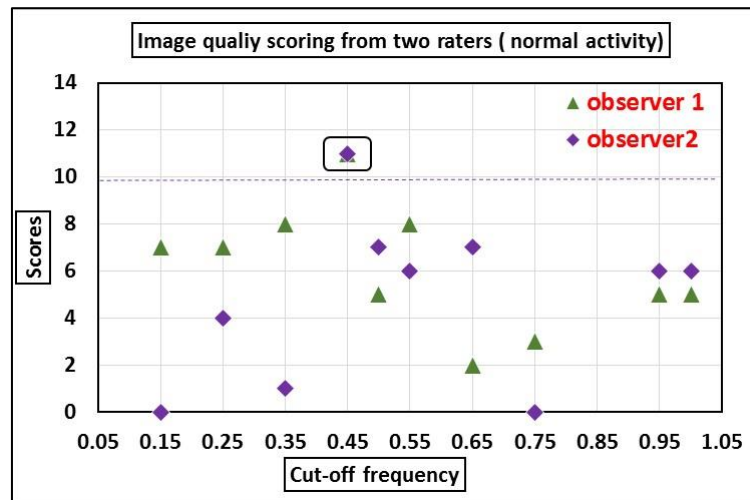


Figure 4.13 Scatter plot of image quality scoring Vs cut-off frequency (normal activity)

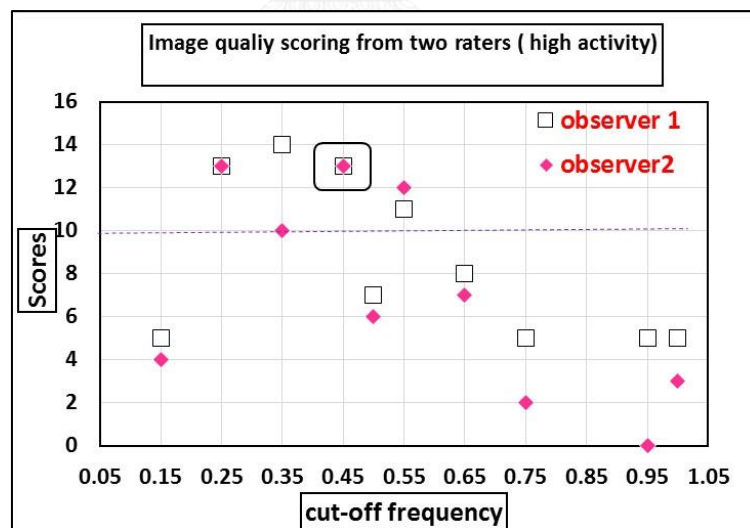


Figure 4.14 Scatter plot of image quality scoring Vs cut-off frequency (high activity)

According to the qualitative scoring, the optimal parameters were set as highest score with related present contrast and noise level. Table 4.14 and 4.15 shows the result of parameters for each activity concentration. The following parameters were got highest score from two observers' interpretation.

Table 4.14 The result of parameters according to qualitative scoring (OSEM)

OSEM	Iteration	Subsets	Update Number	FWHM of Gaussian Filter	%Contrast	Noise	Qualitative Scoring
Low Activity Concentration	6 - 10	8	48 - 80	5-mm	62.76 – 69.14	12.42-15.7	12/14
Normal Activity Concentration	4 - 12	8	32 - 96	5-mm	70.24 – 80.55	9.5 -15.4	13/14
High Activity Concentration	4- 14	8	32 - 112	5-mm	72.31 – 83.52	7.0 – 16.0	14/14

Table 4.15 The result of parameters according to qualitative scoring

FBP	Cut-off Frequency (cycles/pixel)	Order	%Contrast	Noise	Qualitative Scoring
Low Activity Concentration	0.35	10	53	11.8	11/14
Normal Activity Concentration	0.45	10	62	11	11/14
High Activity Concentration	0.25 & 0.45	10	61 & 68	9 &10.7	13/14

According to the results from table 4.14 and 4.15, the optimal protocol can be summarized for each activity concentration based on quantitative measurement and qualitative scoring of 3D-OSEM reconstruction and FBP reconstruction (Table 4.16 and 4.17).

Table 4 16 Summary of optimized protocol for each activity concentration (OSEM)

Activity concentration (kBq/cc)	Iteration number	Subsets (fixed)	Iterative update	FWHM of Gaussian Filter	Chang's Correction (μm^{-1})	Percent Contrast (%)	Noise	Qualitative Score
Low Activity Concentration (46 kBq/cc)	8	8	64	5-mm	0.12	66	14.60	12/14
Normal Activity Concentration (92 kBq/cc)	10	8	80	5-mm	0.12	78	14.00	13/14
High Activity Concentration (138 kBq/cc)	12	8	96	5-mm	0.12	84	13.60	14/14

Table 4.17 Summary of optimized protocol for each activity concentration (FBP)

Activity concentration (kBq/cc)	Cut-off frequency (cycles/pixel)	Order (fixed)	Chang's Correction (μm^{-1})	Percent Contrast (%)	Noise	Qualitative Score
Low Activity Concentration (46 kBq/cc)	0.35	10	0.14	53	11.80	11/14
Normal Activity Concentration (92 kBq/cc)	0.45	10	0.14	62	11.00	11/14
High Activity Concentration (138 kBq/cc)	0.45	10	0.14	68	10.70	13/14

Figure 4.15 is the summarized images of optimal protocol for each activity concentration.

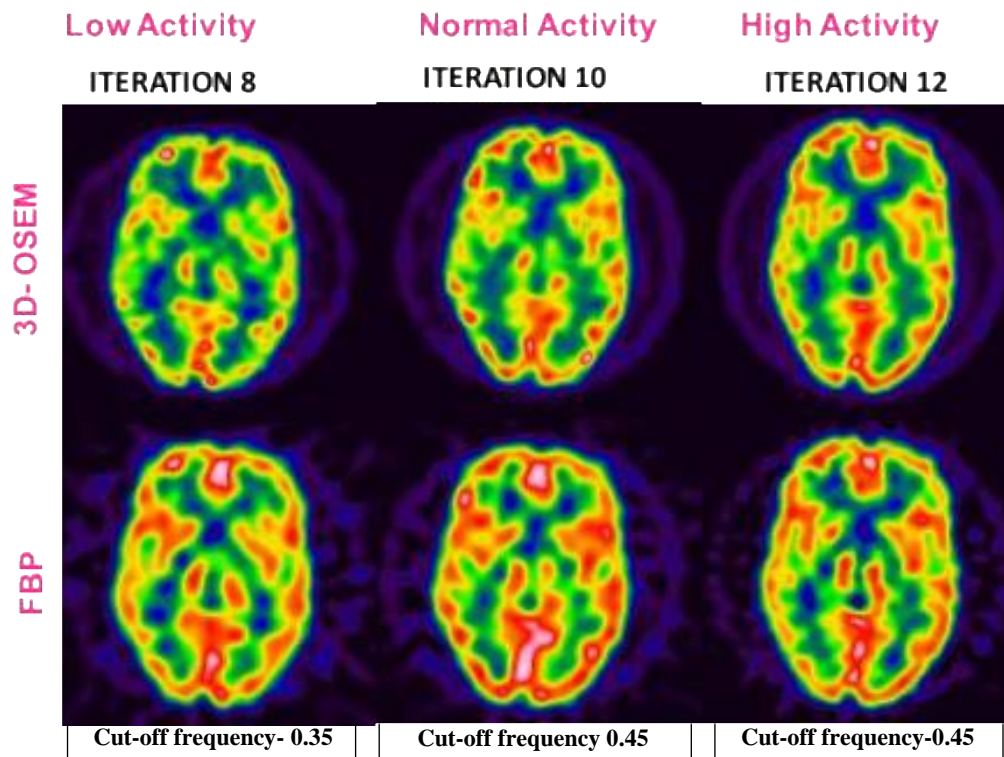


Figure 4.15 Images of summarized optimal protocol for each activity concentration

CHAPTER V

DISCUSSION AND CONCLUSIONS

5.1 Discussion

The result of brain SPECT phantom study showed the reconstruction parameters affect the image quality such as the number of iterations, and choice of filter parameters. The amount of administered activity also affects the image quality. In this study, the image quality was assessed in terms of percent contrast and noise (quantitative) and visual scoring (qualitative) methods for each activity. The updated number and cut-off frequency influenced the image contrast and quantification. The main weak point of brain SPECT imaging is that when the administered activity is low or scanning time is short, the image quality was difficult for diagnosis.

Percent contrast increased with increasing number of iterations and cut-off frequency. The percent contrast and noise of trend results (described in chapter 4) were linear for all activities. When the number of iterations and cut-off frequency were reached at certain point, the percent contrast was plateau. But the noise still increased especially in FBP reconstruction images. High contrast is needed for an accurate diagnosis and assessment of image quality. Therefore, the iterations update number and cut-off frequency must be determined by considering the trade-off between the image contrast, noise and visual scoring.

From the quantitative measurement, when the number of iterations was increased from 1 -15 in OSEM reconstruction, percent contrast and noise were increased from 51 - 72 % and 8 - 20.80 for low activity, 60.13 - 81.25 % and 6.05 - 18.40 for normal activity and 66.67 - 83.72 % and 4.60 - 17.00 for high activity concentration. For the FBP of cut-off frequency increased from 0.15 to 1 cycles/pixel, percent contrast and noise were increased from 46.27 - 58.49 % and 10.20 - 23.00 for low activity, 52.63 - 67.48 % and 8.70 - 21.80 for normal activity and 59.55 - 72.17 % and 8.00 - 17.00 for high activity concentration respectively.

The visual assessed image quality of criteria (as described in chapter 3) were chosen with respect to provide information on image quality of the including parts of the brain that is most often of interest in rCBF SPECT. Five of the seven criteria used correspond to the visibility and discernibility of certain anatomical structures, while the other two criteria correspond to the overall image quality. Scoring ≥ 10 points of total score was acceptable image quality. We determined the scoring ≥ 10 points by considering trade-off between certain anatomical structures and overall image quality.

In OSEM reconstruction method, image quality scoring was the same after iteration number 6 (iterative update of 48) for each activity. For FBP reconstruction, after cut-off frequency of 0.45cycles/pixel, the scoring was significantly reduced. At the lower cut-off frequency, the images blurred because of the filter smoothed edge of images blur. At higher cut-off frequency, the images were grainy and noisy, also making the detection difficult. According to the qualitative scoring, the parameters of OSEM in low activity was 6-10 iterations with 8-subsets (48-80 update number), 4-12 iterations and 8-subsets (32-96 updates) for normal activity and 4-14 iterations and 8-subsets (32-112 updates number) for high activity were satisfied with highest score

among iterations (1-15) number. The optimal parameters of FBP were cut-off frequency 0.35 cycles/pixel and order 10 in low activity, 0.45 cycles/pixel and order 10 in normal activity and 0.35 and 0.45 cycles/pixel and order 10 for high activity were achieved highest score between cut-off frequencies (0.15-1) cycles/pixel respectively.

Groch and Erwin (2000) (15) showed that the most suitable filter for ^{99m}Tc -HMPAO brain SPECT study is the Butterworth filter with order 10 and 0.45 Nq cut-off frequency. This filter gave the best compromise between noise and resolution. Our study agreed well with this article for normal activity and high activity concentration. Our study was 0.35 cycles/pixel for the low activity concentration. This article used the same activity of clinical patient studies. Our study used low activity concentration and over cutoff frequency of 0.35, the image becomes noisy because of low counts statistic.

Brambilla Met.al (2004) (16) reported that OSEM algorithm with Gaussian post filter and comparison with FBP in ^{99m}Tc SPECT study in terms of contrast, noise and spatial resolution by using Jaszczak phantom. For FBP, Butterworth filter of order 5 and cut-off frequency of 0.5 and 0.7 cycles/pixel. OSEM were halted after 5, 10 and 15 iterations with 4, 8 and 16 subsets. The contrast and noise increases with increasing number of iterations and saturated at 80 iterations update. Contrast at 80 iterations update is higher than FBP. This article determined on Jaszczak image quality phantom and Jaszczak phantom determined the percent contrast on different sizes of cold spheres and our study was determined directly on Hoffman 3D brain phantom of gray and white matter percent contrast and noise. The iterations number can be different however our result revealed with this article of OSEM percent contrast was superior to FBP reconstruction.

Dickson et.al (2009) (17) reported reconstruction of DaTSCAN brain studies using OSEM iterative reconstruction (2 – 10 iterations and 10- subsets) offers better image quality and more accurate quantification than filtered back-projection data. OSEM reconstruction using update number 100 will provide the best image quality and quantification in brain SPECT imaging. They studied with a striatal brain phantom filled with ^{123}I and different radiopharmaceuticals using striatal to background quantification ratios. Our study performed with $^{99m}\text{TcO}_4$.

Alzimami K et.al (2008) (2) reported evaluation of 3D OSEM, and a comparison with FBP in ^{99m}Tc SPECT images with Jaszczak phantom. The parameters of cut-off frequency varied from 0.4 – 0.8 cycles/pixel with fixed order 15 and OSEM with 1, 4, 8, 12 and 15 iterations and 8-subsets for contrast and noise quantification. Contrast was halted at iterations number 4, 8 and 12 and cut-off frequency 0.5, 0.6 and 0.7 as shown in figure (1). 3D OSEM is the best choice especially for low count study as 3D OSEM is significantly ($P < 0.01$) better than FBP in terms of noise (figure 5.1). OSEM 3-D allows the reconstruction of all slices simultaneously, thus improving count statistics.

According to the above literature studies, many factors affect to the image quality in brain SPECT imaging such as type of filter, number of cut-off frequency, number of iterations and subsets, amount of administered activity and number of detected counts.

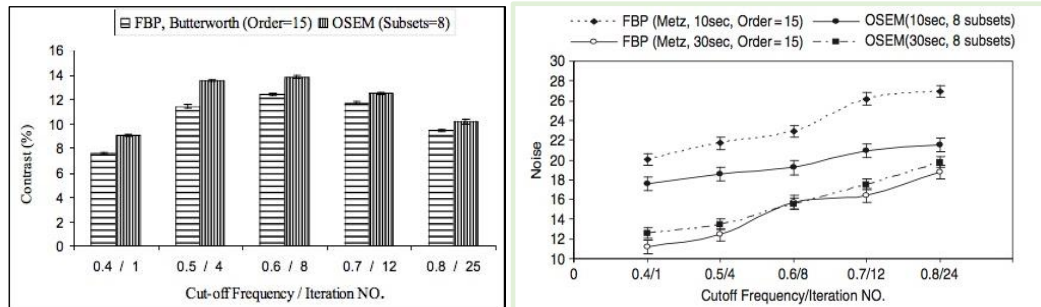


Figure 5.1 Percent contrast and noise comparison between FBP and OSEM reconstruction

Our study agreed with the above studies using with Jaszczak phantom, striatal brain phantom and clinical data for image quality and quantification. Hoffman brain phantom had been used with the advantage of that the percent contrast and noise can be determined directly on brain region of gray and white matter. The percent contrast between gray and white matter plays an important role in diagnostic accuracy in brain SPECT imaging.

The iterative reconstruction, OSEM method has been used more than FBP. In this study, percent contrast evaluation is higher and noise result showed lower in OSEM than FBP. By comparison with OSEM and FBP reconstruction according to quantitative evaluation, OSEM method is better percent contrast than FBP. From qualitative visual scoring, FBP with optimal parameter can be interpreted even in low activity concentration. These optimal parameters can be implemented in clinical brain SPECT studies.

Figures (5.2 - 5.7) represent the images of the optimal reconstruction parameters of each activity concentration in OSEM and FBP reconstruction method.

Figure 5.2 represents the images of optimal reconstruction parameters with iteration 8 and subsets 8 (iterative updates 64) in low activity concentration in OSEM method.

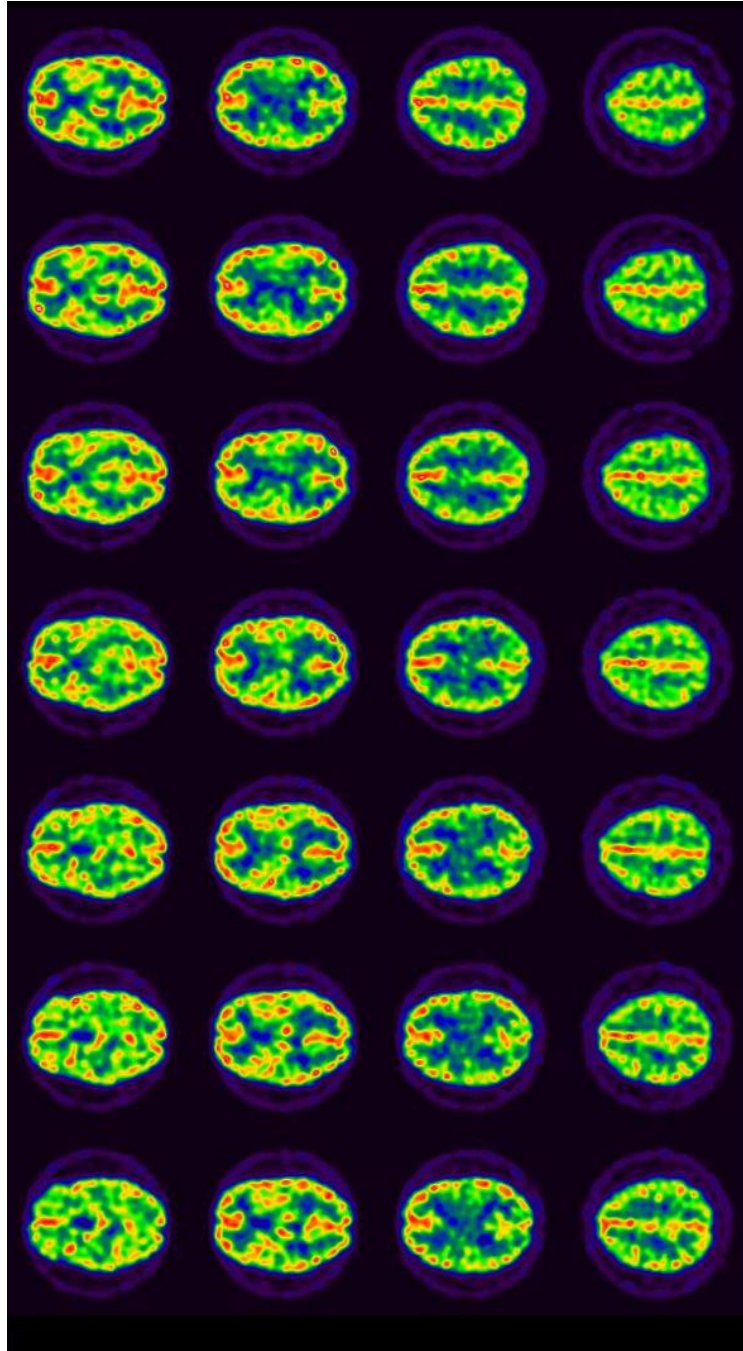


Figure 5.2 The images of optimized parameters in low activity concentration (3D-OSEM)

Figure 5.3 represents the images of optimal reconstruction parameters with iteration 10 and subsets 8 (iterative updates 80) in normal activity concentration in OSEM method.

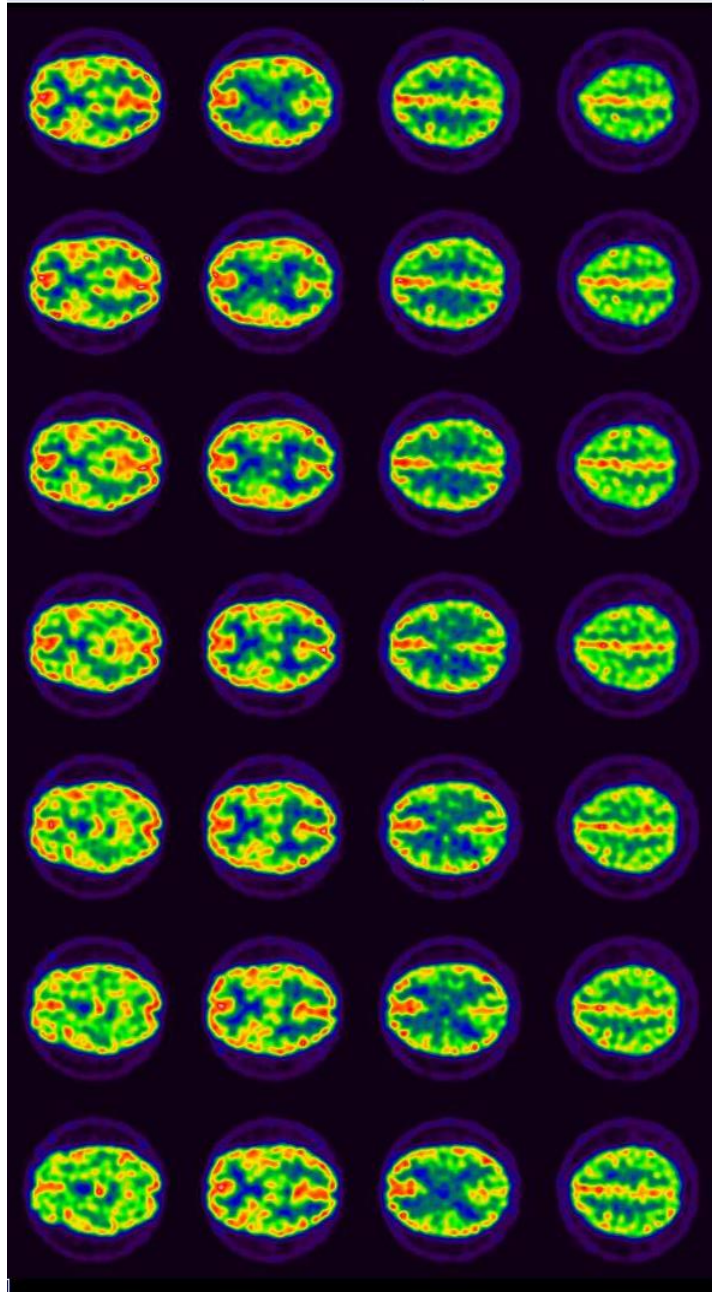


Figure 5.3 The images of optimized parameters in normal activity concentration (3D-OSEM)

Figure 5.4 represents the images of optimal reconstruction parameters with iteration 12 and subsets 8 (iterative updates 96) in high activity concentration in OSEM method.

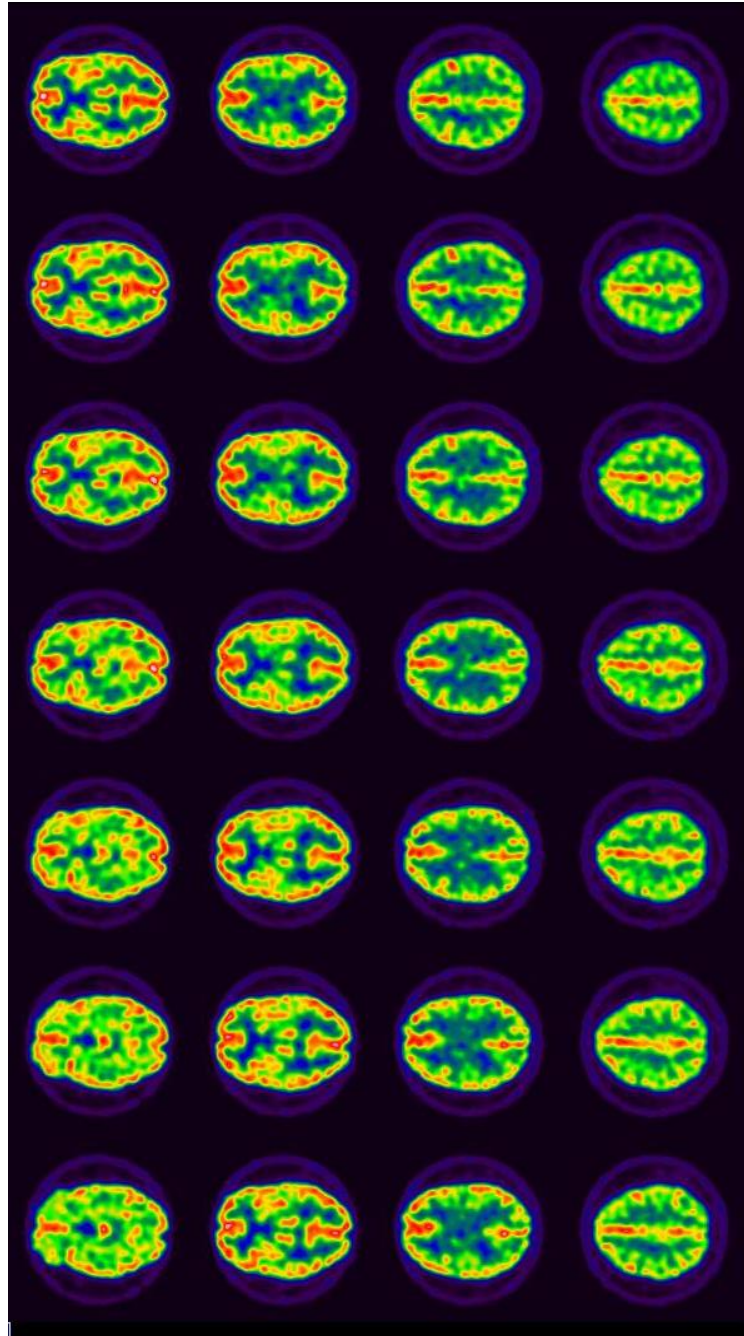


Figure 5.4 Images of optimized parameters in high activity concentration (3D-OSEM)

Figure 5.5 represents the images of optimal reconstruction parameters with cut-off frequency 0.35cycles/pixel and order 10 in low activity concentration FBP method.

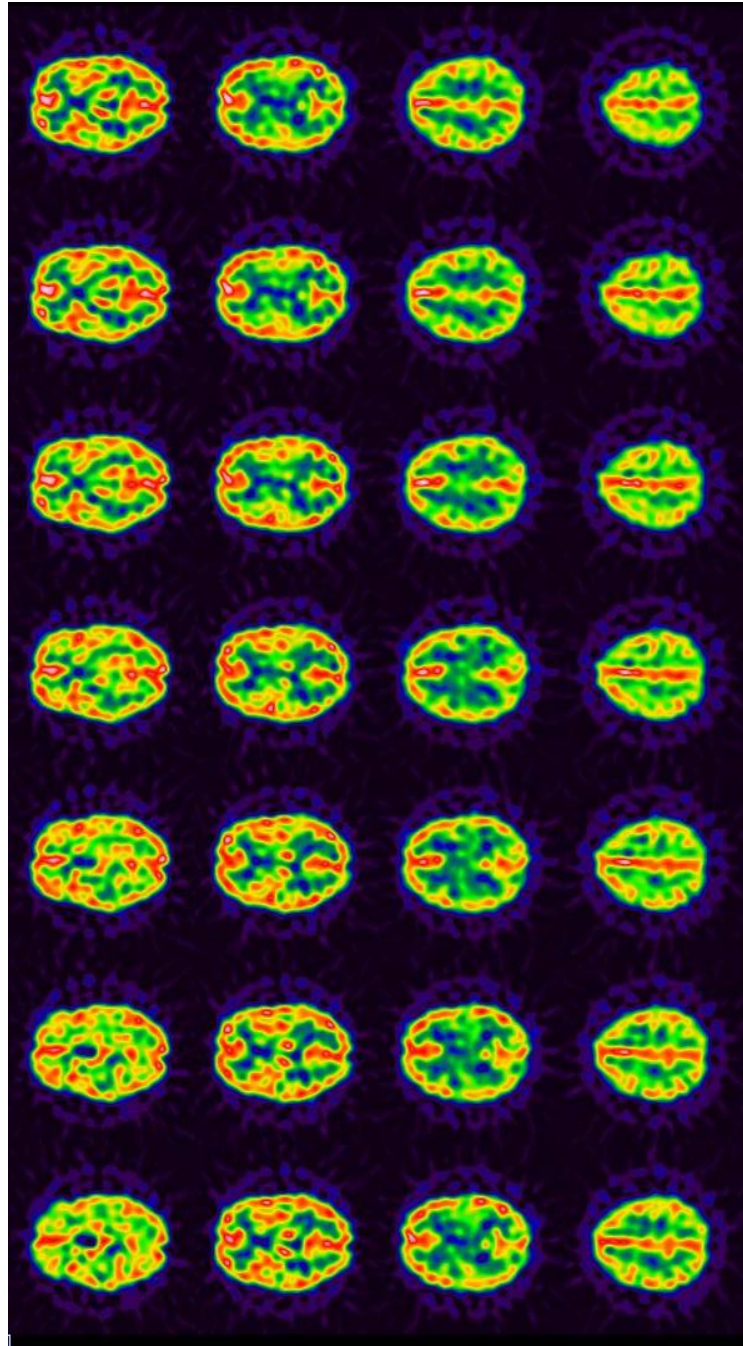


Figure 5.5 Images of optimized parameters in low activity concentration (FBP)

Figure 5.6 represents the images of optimal reconstruction parameters with cut-off frequency 0.45cycles/pixel and order 10 in normal activity concentration FBP method.

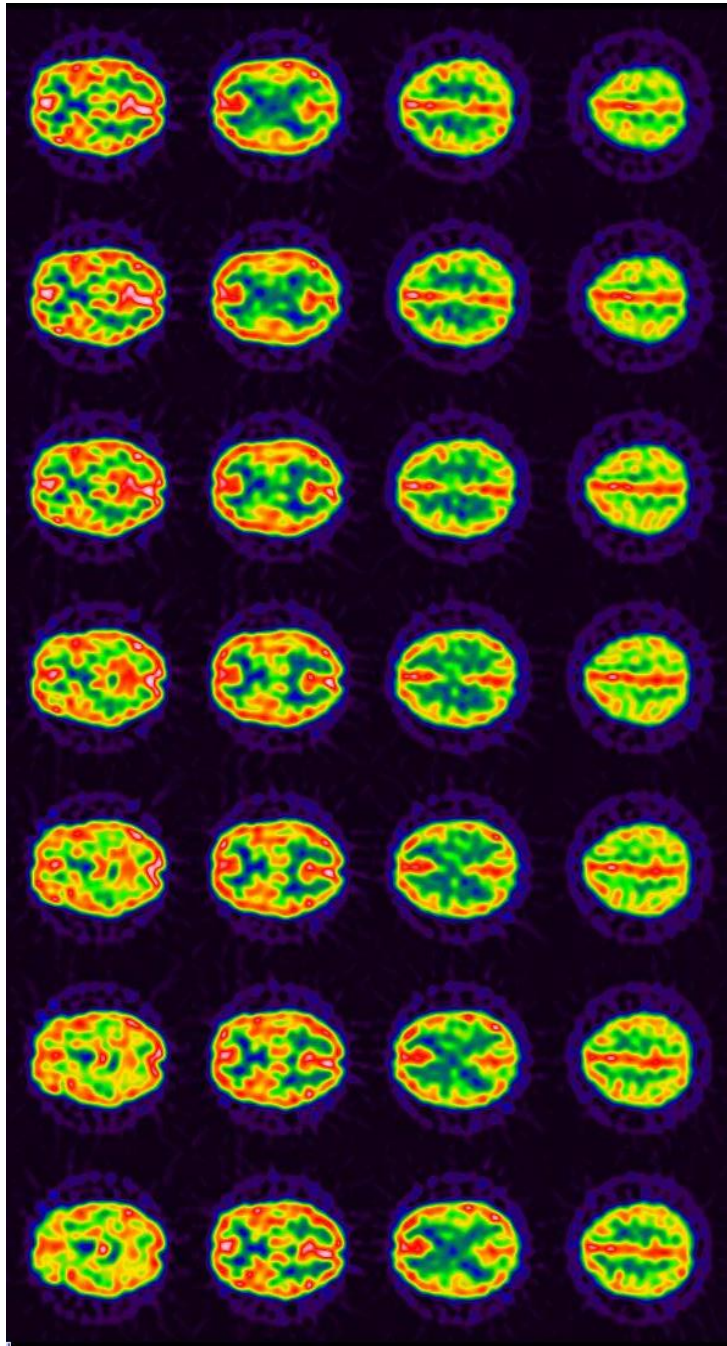


Figure 5.6 Images of optimized parameters in normal activity concentration (FBP)

Figure 5.7 represents the images of optimal reconstruction parameters with cut-off frequency 0.45 cycles/pixel and order 10 in high activity concentration FBP method.

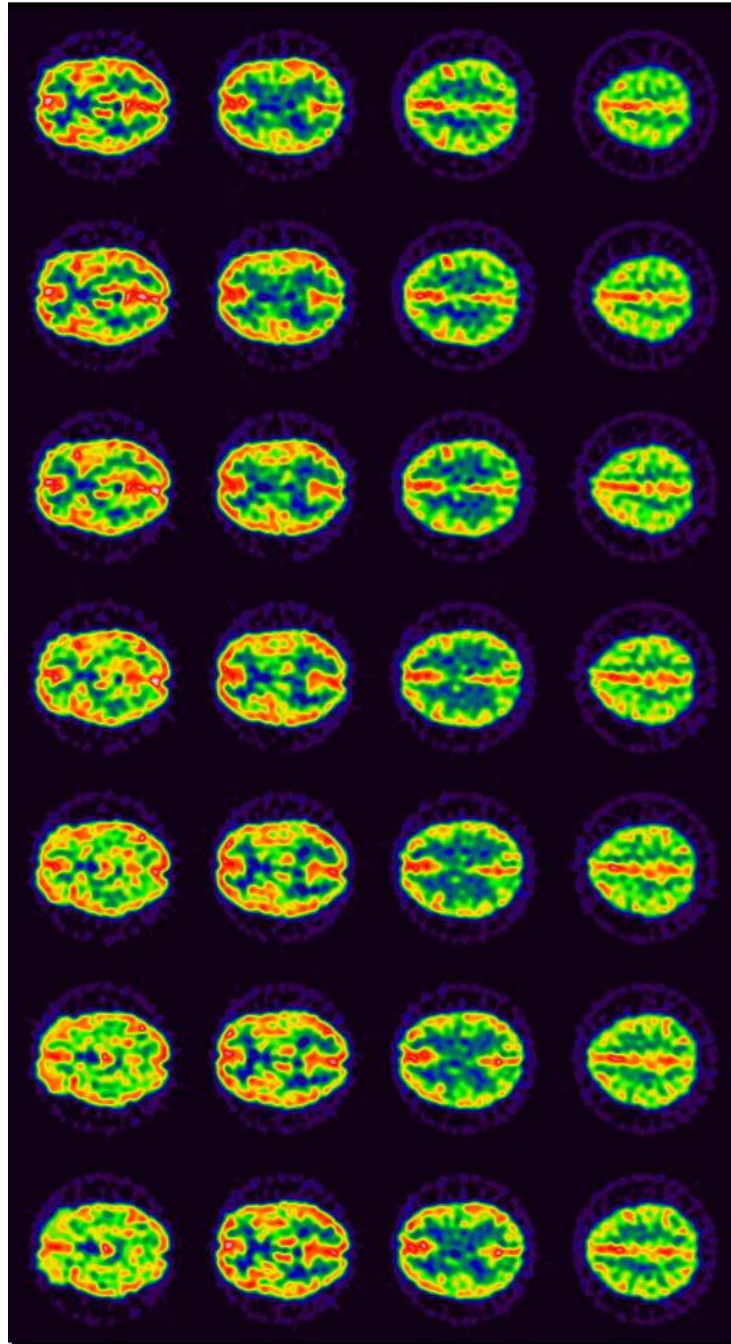


Figure 5.7 Images of optimized parameters in high activity concentration (FBP)

5.2 Conclusions

The iterative reconstruction, OSEM method has been used more than FBP. Noise evaluation is lower in OSEM than FBP. For OSEM reconstruction method, the optimal reconstruction parameters of low activity concentration (46 kBq/cc) were 8-iteration and 8-subsets (64-iterative updates), FWHM of Gaussian filter 5-mm and Chang' attenuation coefficient of 0.12cm^{-1} . The related percent contrast and noise were 66.00 % and 14.60 and qualitative score of 12. For normal activity concentration (92kBq/cc) was 10-iteration and 8-subsets (80-iterative updates), FWHM of Gaussian filter 5-mm and Chang' attenuation coefficient of 0.12-cm^{-1} . The related percent contrast and noise were 78.00 % and 14.00 and qualitative score of 13 respectively. For high activity concentration (138 kBq/cc) was 12-iteration and 8-subsets (96-iterative updates), FWHM of Gaussian filter 5-mm and Chang' attenuation coefficient of 0.12cm^{-1} . The related percent contrast and noise were 84.00 % and 13.60 and qualitative score of 14.

For FBP reconstruction method, the optimal reconstruction parameters of low activity concentration (46 kBq/cc) were 0.35 cycles/pixel, order 10 of Butterworth filter and Chang' attenuation coefficient of 0.14cm^{-1} . The related percent contrast and noise were 52.92 % and 11.80 and qualitative score of 11. For normal activity concentration (92 kBq/cc) was 0.45 cycles/pixel, order 10 of Butterworth filter and Chang' attenuation coefficient of 0.14cm^{-1} . The related percent contrast and noise were 62.19 % and 11.00 and qualitative score of 11. For high activity concentration (138 kBq/cc) was 0.45 cycles/pixel, order 10 of Butterworth filter and Chang' attenuation coefficient of 0.14cm^{-1} . The related percent contrast and noise were 68.61 % and 10.70 and qualitative score of 13 respectively.

Our study showed that image quality can be improved by optimization reconstruction parameters even in low activity concentration. Percent contrast evaluation is higher and noise result showed lower in OSEM than FBP. By comparison with OSEM and FBP reconstruction according to quantitative evaluation, OSEM method is better percent contrast than FBP. From qualitative visual scoring, FBP with optimal parameters can be interpreted even in low activity concentration.

These optimizing parameters can be implemented in routine brain SPECT clinical studies.

5.3 Limitations

There are some limitations in this study. For OSEM reconstruction, varied only in iterations number and fixed FWHM of Gaussian filter. Varying the filter also affect the image quality evaluation. Without the analysis of brain software, the ROI in brain region was drawn manually. For consistency of region drawing, the same size of ROI throughout the regions had been used.

5.4 Recommendation

The image quality of brain SPECT imaging was done with Siemens Symbia True Point T6 SPECT/CT system. These optimal parameters could be further applied and determined in GE SPECT/CT system.

REFERENCES

- [1] Buck AK, Nekolla S, Zeigler S, Beer A, Krause BJ, Herrmann K, et al. SPECT/CT. *J Nucl Med.* 2008;49: 19-1305.
- [2] Alzimami K, Sassi S, Spyrou NM. An evaluation of 3D OSEM, and a comparison with FBP in 99mTC SPECT images. *Proc World Congr Eng.* 2008;1:1-5.
- [3] Accorsi R. Brain single-photon emission CT physics principles. *AJNR Am J Neuroradiol.* 2008;29:56-1247.
- [4] Morano GN, Seibyl JP. Technical overview of brain SPECT imaging: improving acquisition and processing of data. *J Nucl Med Technol.* 2003;31: 5-191.
- [5] Kim HJ, Karp JS, Mozley PD, Yang SO, Moon DH, Kung HF, et al. Stimulating technetium-99m cerebral perfusion studies with a three-dimensional Hoffmann brain phantom: collimator and filter selection in SPECT neuroimaging. *Ann Nucl Med.* 1996;10: 60-153.
- [6] Lyra M, Ploussi A. Filtering in SPECT Image Reconstruction. *International journal of biomedical imaging.* 2013;6:291-297.
- [7] Catafau AM. Brain SPECT in clinical practice. Part I: perfusion. *J Nucl Med.* 2001;42: 71-259.
- [8] Sofia K. Optimization of activity level in rCBF SPECT using the observer study visual grading regression [Master of Science Dissertation]. Lund, Sweden: Lund University. 2012.
- [9] Cherry SR, Sorenson JA, Phelps ME. *Physics in Nuclear Medicine.* Fourth ed. Saunders. 2012; 544 p.
- [10] Mariani G, Flotats A, Israel O, Kim EE, Kuwert T. *Clinical Applications of SPECT/CT: New Hybrid Nuclear Medicine Imaging System-IAEA-TECDOC-1597.* Vienna. 2008; 62 p.
- [11] Asl NM, Sadremomtaz A. Analytical image reconstruction methods in emission tomography *J Biomed Sci Eng.* 2013;6:7-100.
- [12] Bruyant PP. Analytic and iterative reconstruction algorithms in SPECT. *J Nucl Med.* 2002;43: 58-1343.
- [13] Hoffman 3-D Brain Phantom™. Available from: <http://www.biodex.com/nuclear-medicine/products/phantoms/hoffman-3-d-b>.

- [14] Gwet KL. Computing inter-rater reliability and its variance in the presence of high agreement. *Br J Math Stat Psychol*. 2008;61:29-48.
- [15] Groch MW, Erwin WD. SPECT in the year 2000: basic principles. *J Nucl Med Technol*. 2000;28:44-233.
- [16] Brambilla M, Cannillo B, Dominiotto M, Leva L, Secco C, Inglese E. Characterization of ordered-subsets expectation maximization with 3D post-reconstruction Gauss filtering and comparison with filtered backprojection in ^{99m}Tc SPECT. *Ann Nucl Med*. 2005;19:75-82.
- [17] Dickson JC, Tossici-Bolt L, Sera T, Erlandsson K, Varrone A, Tatsch K, et al. The impact of reconstruction method on the quantification of DaTSCAN images. *Eur J Nucl Med Mol Imaging*. 2010;37:23-35.



APPENDIX A

Quality Control of SPECT/CT

1. Part of CT (Daily)

Purpose

- To check quality of x-ray beam by using water phantom,
- Pixel noise of image (standard deviation)
 - Tube voltage (measure directly on the x-ray tube)

Material

Siemens water phantom

Methods

1. Warm up CT tube before use on patients. This is necessary because the CT tube needs to be at a particular operating temperature before it performs properly.
2. Then calibrate blank scan on CT for kVp 110 and mAs 150.
3. Table A1 shows the one month results of daily QC.

Tolerance level for kVp

For 80 kVp (71.80-87.80)
For 110 kVp (98.80-120.80)
For 130 kVp (116.60-142.60)

Table A 1. Daily quality control of CT for one month results

	Check Up	Set kVp	Measured Voltage (kVp)	Image Noise (HU)	Temp (°C)	Humidity (%)	Physical
3.Oct.16	P	110	109.8	16.22	23.0	67.0	P
4.Oct.16	P	110	109.8	16.19	23.0	63.0	P
5.Oct.16	P	110	109.8	16.31	23.0	61.0	P
6.Oct.16	P	110	109.8	16.31	23.0	61.0	P
7.Oct.16	P	110	109.8	16.20	23.0	61.0	P
10.Oct.16	P	110	109.8	16.40	23.0	65.0	P
11.Oct.16	P	110	109.8	16.34	24.0	61.0	P
12.Oct.16	P	110	109.8	16.38	24.0	65.0	P
13.Oct.16	P	110	109.8	16.26	24.0	62.0	P
14.Oct.16	P	110	109.8	16.42	24.0	62.0	P
17.Oct.16	P	110	109.8	16.23	24.0	54.0	P
18.Oct.16	P	110	109.8	16.31	24.0	54.0	P
19.Oct.16	P	110	109.8	16.35	24.0	52.0	P
20.Oct.16	P	110	109.8	16.24	24.0	54.0	P
21.Oct.16	P	110	109.8	16.31	23.0	57.0	P
25.Oct.16	P	110	109.8	16.31	23.0	54.0	P
26.Oct.16	P	110	109.8	16.30	23.0	53.0	P
27.Oct.16	P	110	109.8	16.54	23.0	59.0	P
28.Oct.16	P	110	109.8	16.32	23.0	59.0	P
31.Oct.16	P	110	109.8	16.31	23.0	57.0	P

2. Part of SPECT

2.1 Weekly intrinsic uniformity calibration

Purpose

To check the intrinsic response of scintillation camera to spatially uniform flux of incident photons over the field of view.

Materials

1. Point source of 0.74 MBq (20 uCi) Tc-99m solution in suitable container.
2. Source holder for point source

Methods

1. Remove the collimator from the detector head. Align the detector head and source holder.
2. Mount the source in the source holder.
3. Use weekly QC protocol for peaking, tuning and acquiring 30M counts.

Differential uniformity: the amount of count density changes per defined unit distance when the detector's incident gamma radiation is homogenous flux over the field of measurement.

$$\text{Differential Uniformity} = \pm 100 * ((\text{Max} - \text{Min}) / (\text{Max} + \text{Min}))$$

Integral Uniformity: a measure of the maximum count density variation over a defined large area of the scintillation detector for a uniform input gamma flux to the useful field of view of the camera.

$$\text{Integral Uniformity} = \pm 100 * ((\text{Max} - \text{Min}) / (\text{Max} + \text{Min}))$$

Results:

Peak of both detectors for Tc-99m is 141.35Kev
Tuning is passed for both detectors.

Table A 2. Weekly intrinsic uniformity results for one month (October-2016)

Date	Uniformity Detector 1				Uniformity Detector 2			
	CFOV		UFOV		CFOV		UFOV	
	IU	DU	IU	DU	IU	DU	IU	DU
Mon 3-Oct	1.76	1.19	2.07	1.52	1.76	1.19	2.04	1.38
Mon 10-Oct	1.84	1.45	1.87	1.45	1.74	1.19	1.93	1.39
Mon 17-Oct	1.49	1.07	2.38	1.63	2.03	1.27	1.73	1.4
Tue 25-Oct	1.65	1.23	2.12	1.5	1.83	1.24	2.01	1.28

NEMA tolerance level for Uniformity

	CFOV	UFOV
Integral	± 2%	± 2.5%
Differential	± 1.5%	± 2 %

Comment: Pass**2.2 Energy window check (Peaking)****Purpose**

To check the correct energy setting (i.e. a photo peak in the center of the energy window).

Materials and Methods

The same as the monthly intrinsic uniformity Use daily QC protocol for peaking and acquiring 30M counts.

Results:**Table A 3.** Daily energy peak results for one month (October-2016)

Date	Energy peak(Kev)	
	Detector 1	Detector 2
3.10.2016	141.35	141.35
4.10.2016	141.35	141.35
5.10.2016	141.35	141.35
6.10.2016	141.35	141.35
7.10.2016	141.35	141.35
10.10.2016	141.35	141.35
11.10.2016	141.35	141.35
12.10.2016	141.35	141.35
13.10.2016	141.35	141.35
14.10.2016	141.35	141.35
17.10.2016	141.35	141.35
18.10.2016	141.35	141.35
19.10.2016	141.35	141.35
20.10.2016	141.35	141.35
21.10.2016	141.35	141.35
25.10.2016	141.35	141.35
26.10.2016	141.35	141.35
27.10.2016	141.35	141.35
28.10.2016	141.35	141.35
31.10.2016	141.35	141.35

2.3 Center of rotation

Purpose

To check the center of rotation offset, alignment of the camera and head tilt with respect to axis of rotation.

Materials

Five ^{99m}Tc point sources

MHR (multiple head alignment rotation)/COR phantom

Methods

Five point sources with activity approximates 37 MBq was prepared on the vial supplied with camera system. The vial source on MHR/COR phantom was mounted and placed on top of the patient bed as shown in figure. The detectors with LEUR collimator to 180-degree configuration and make sure those 5 point sources are in center of field of view. The detector was rotated to 90 degree to check that 5-point source is at center. MHR/COR protocol was used to perform acquisition with non-uniformity correction. MHR/COR calibration was performed on detector 90-degree configuration.

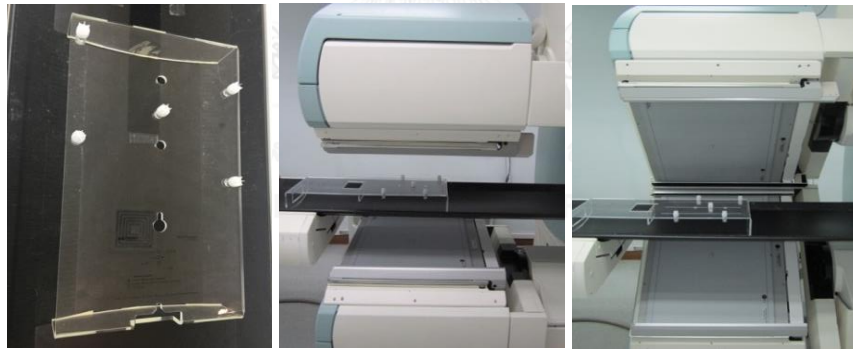


Figure A 1. MHR/COR phantom with 5-point sources

Results

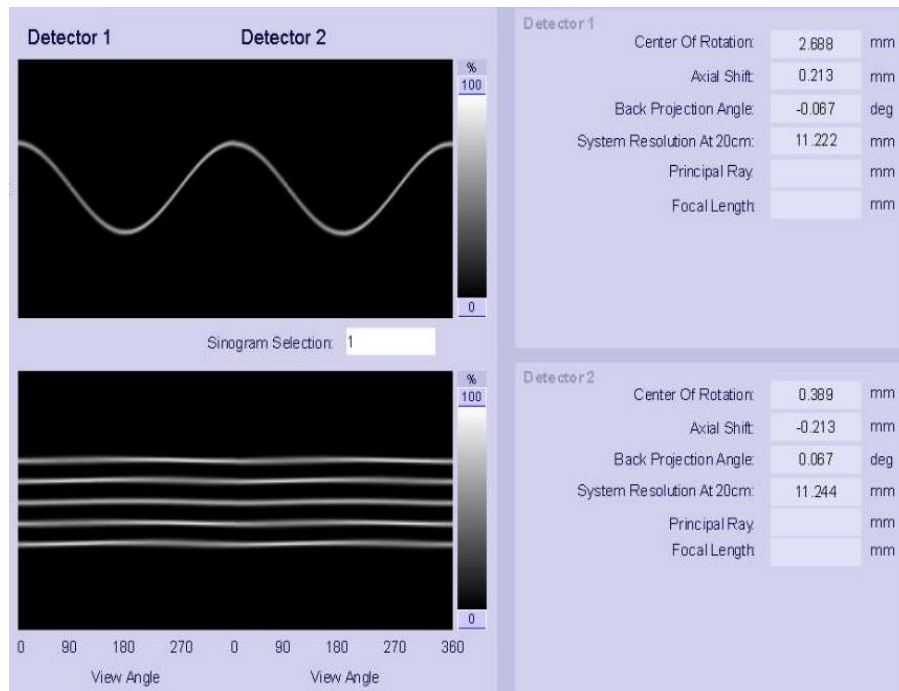
Table A 4. MHR/COR for 180 - degree detector parallel configuration result

	Detector 1	Detector 2	Specification
COR	2.688 mm	0.389 mm	< 10 mm
Axial shift	0.213 mm	-0.213 mm	<5mm
Back projection angle	- 0.067 degree	0.067 degree	< 0.8
System resolution at 20cm	11.222 mm	11.244 mm	

Table A 5. MHR/COR for 180- degree detector parallel verification result

	Detector 1	Detector 2	Specification
COR	-0.094	-0.0728 mm	$\leq 2\text{mm}$
Axial shift	0.049 mm	-0.049 mm	
Back projection angle	0.019 degree	-0.019 degree	≤ 0.2 degree
System resolution at 20cm	12.224 mm	12.220 mm	

COR 180



COR 180 verification

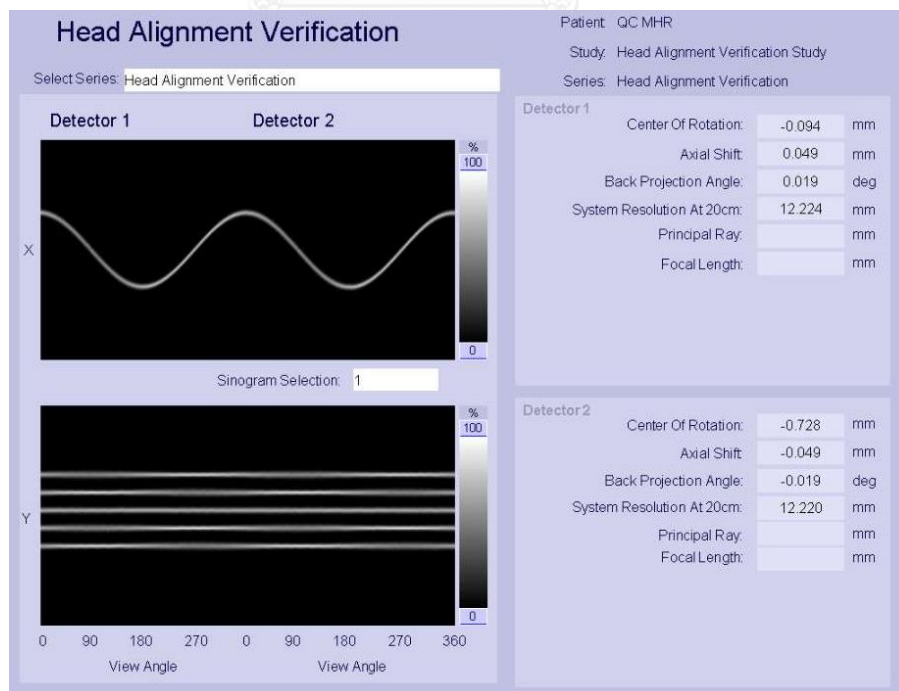


Figure A 1. COR 180 parallel configuration and verification results

Limits of acceptability

The mean value of center of rotation offset should be < 10 mm and the back-projection angle should be < 0.8 . Axial shift should be < 5 mm.

The head alignment verification result should be ≤ 2 mm in the center of rotation and axial area, the back-projection angle should be ≤ 0.2 degree.

Comment: The results are within the limit and pass.

2.4 Image Quality result with Jaszczak Phantom

Purpose To test the SPECT system in clinical studies

Method The deluxe Jaszczak Phantom is filled with water and 740 MBq (20 mCi) of Technetium pertechnetate. The activity concentration of the ^{99m}Tc is 0.1213 MBq/cc. It is then shaken to mix thoroughly. The acquisition protocol is 30 seconds per view of total 128 views; detector configuration is 180-degree. The image matrix size is 128x128, and zoom factor 1 (pixel size 4.8mm) are used. The acquisition time for SPECT scan is 30 minutes as shown in figure. The OSEM and FBP reconstruction is applied with attenuation coefficient of 0.12cm^{-1} . For OSEM reconstruction, iterative 8 and subsets 8 were applied. For FBP, Butterworth filter of 0.48 and order 10 were applied.

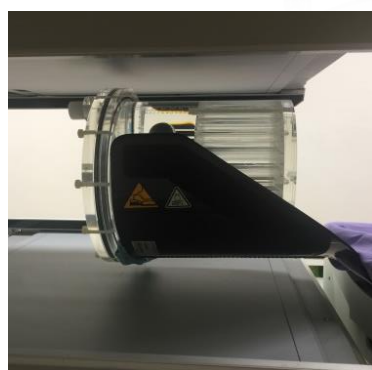


Figure A 2. Jaszczak Phantom Scanning

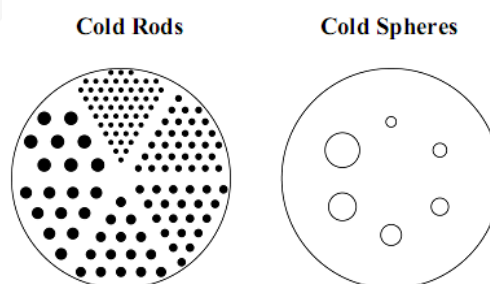


Diagram of Jaszczak phantom

Cold Rods— 12.7, 11.1, 9.5, 7.9, 6.4, 4.8 mm

Cold Spheres – 31.8, 25.4, 19.1, 15.9, 12.7, 9.5mm

%Contrast can be calculated by the following equation

$$\%Contrast = \left[\frac{\text{Avg background counts/pixel} - \text{Avg sphere counts/pixel}}{\text{Avg background counts}} \right]$$

Table A 6. Results from 3D-OSEM reconstruction

JaszczakPhantom Preparation=740MBq		Recon- OSEM	AC=0.12cm ⁻¹	Iteration8 &subset 8
Solid sphere diameter(mm)	Avg Sph Counts/pixel	Avg Bg Count/pixels	Contrast	%Contrast
9.5	512	689	0.25	25
12.7	444.2	708	0.37	37
15.9	374.21	698	0.47	47
19.1	319.54	700	0.55	55
25.4	266.22	712.91	0.63	63
31.8	224.97	722.47	0.69	69

Avg = Average, Sph = Sphere, Bg =Background

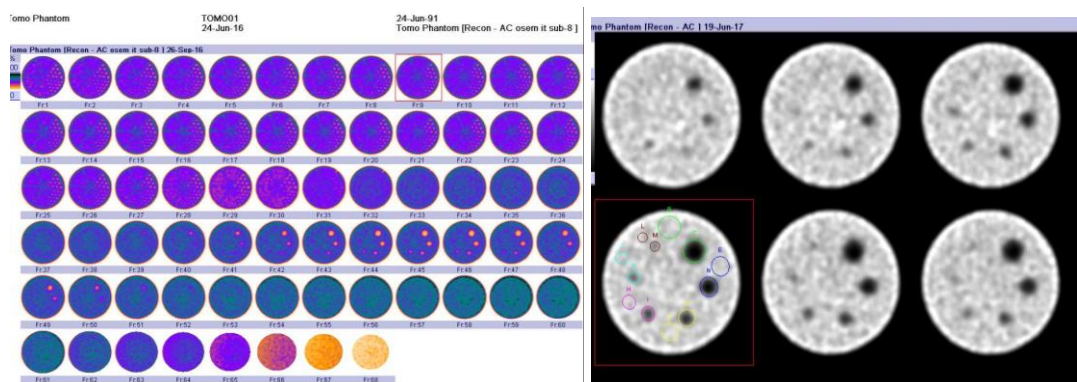
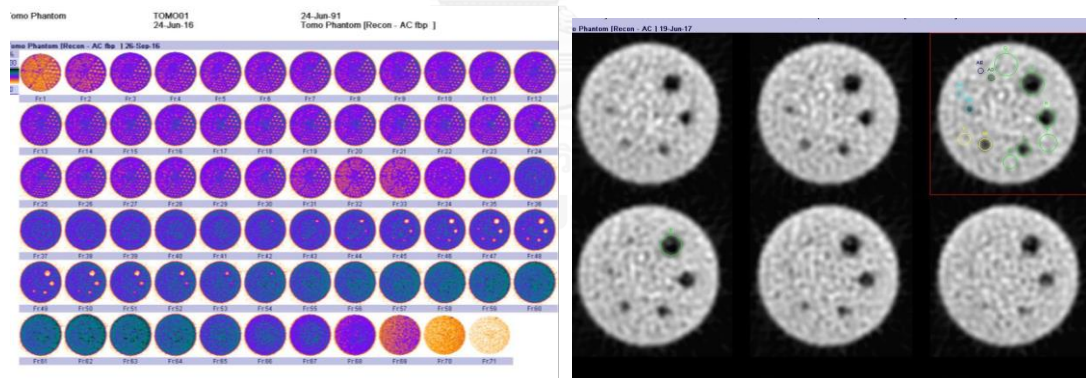


Figure A 3. Jaszczak Images from OSEM reconstruction

Table A 7. Results from FBP reconstruction

JaszczakPhantom Preparation=740MBq		Recon-FBP	AC=0.12cm ⁻¹	Cut-off fc=0.48, order 10
Solid Sphere Diameter(mm)	Avg Sph Counts/pixel	Avg Bg Counts/pixel	Contrast	%Contrast
9.5	622	740	0.15	15
12.7	579	750	0.22	22
15.9	538	758	0.29	29
19.1	490	756	0.36	36
25.4	397	745	0.47	47
31.8	318	760	0.58	58

**Figure A 4.** Jaszczak Images from FBP reconstruction

2.5 System Planar Sensitivity

Purpose

To test the count rate response of a scintillation camera to a radionuclide source of known radioactivity

Materials

A petri dish with 10 cm diameter

A foam with 10 cm height

Methods

1. Fill water 25 cc and ^{99m}Tc activity 273.43MBq (7.39 mCi) into the petri dish.
2. Record the time for preparation to correct the decay.
3. Place the foam on the center of detector and put on petri dish on top.
4. Acquire with the preset counts of 4000 kcounts with LEUR collimator, matrix 256x256, zoom 1, no uniformity correction.
5. Perform the acquisition with both detectors following NEMA (2007) protocol.

Table A 8. Sensitivity Results for LEUR collimator

	Detector I	Detector II	Specification
Total Counts	4000000	4000000	
Scan times	445 -sec	433-sec	
Bkg counts	3658	3482	
Net counts	3996342	3996518	
CPS/mCi	1404.527	1408.060	
CPM/μCi	84.271	84.483	100 CPM/μCi
CPM/MBq	2277.611	2283.341	

Comment: Detector 1 and 2 sensitivities were 84.2716 CPM/ μCi (2277.611 CPM/MBq) and 84.4836 CPM/ μCi (2283.341 CPM/MBq), the results are lower than specification of 100 CPM/ μCi because the detector is close to 10 years since installation. There are deterioration in gamma absorption of detector

APPENDIX B

Figure 1-6 show the brain SPECT images by varying iterations number and cut-off frequency in OSEM and FBP reconstruction methods for each activity concentration.

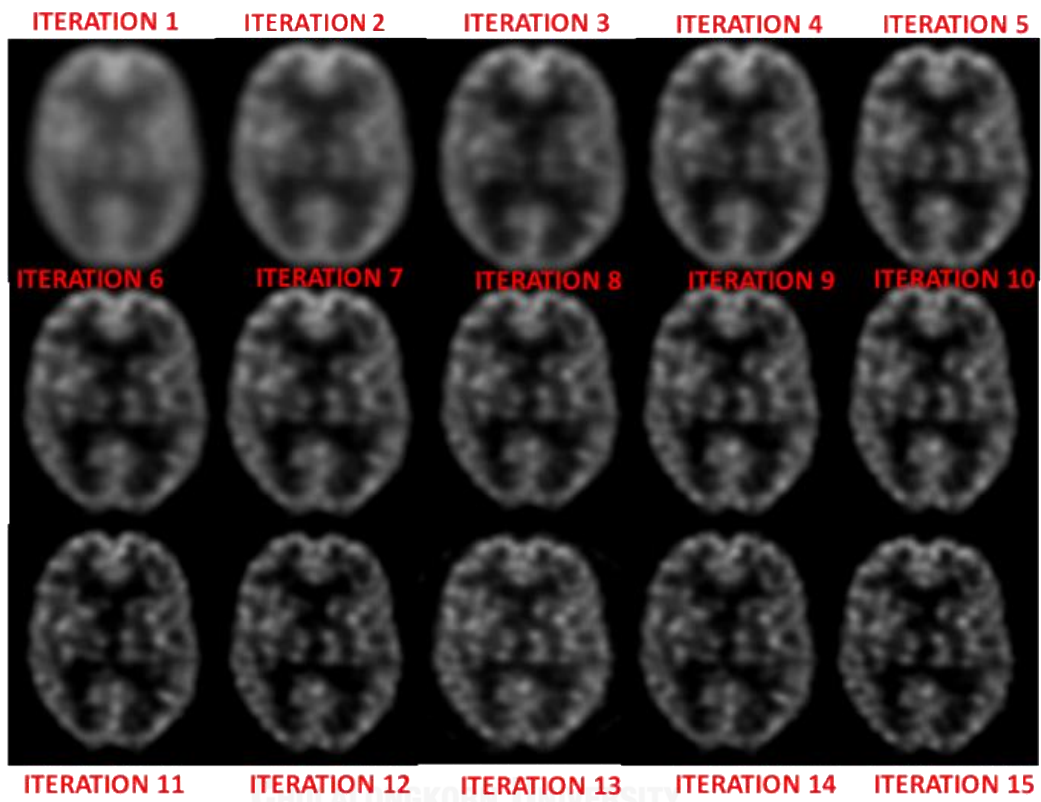


Figure B 1. The brain SPECT images by varying number of iterations in low activity concentration (3D- OSEM)

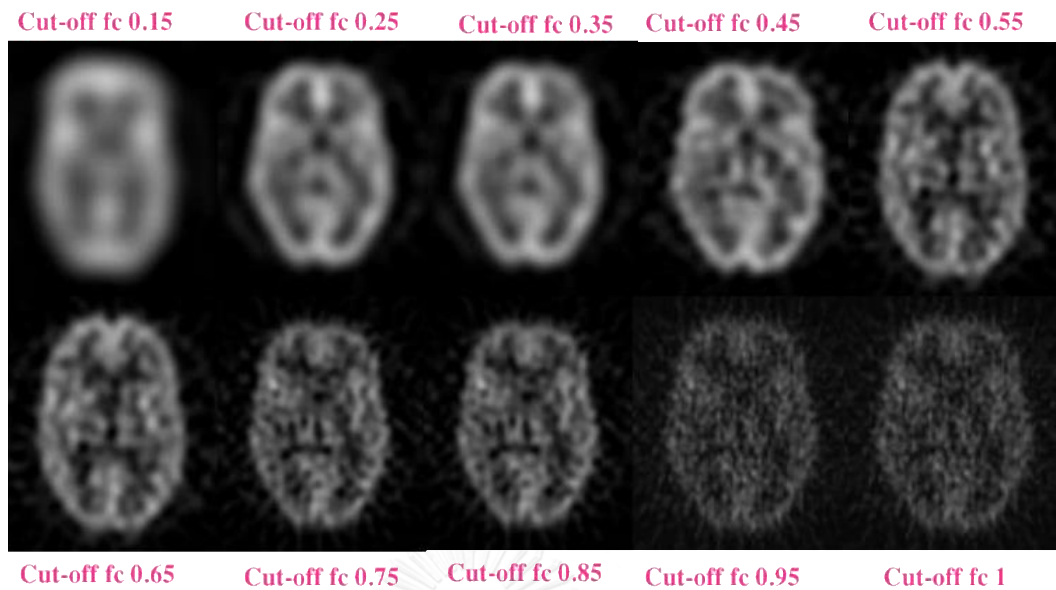


Figure B 2. The brain SPECT images by varying cut-off frequencies in low activity concentration (FBP method)

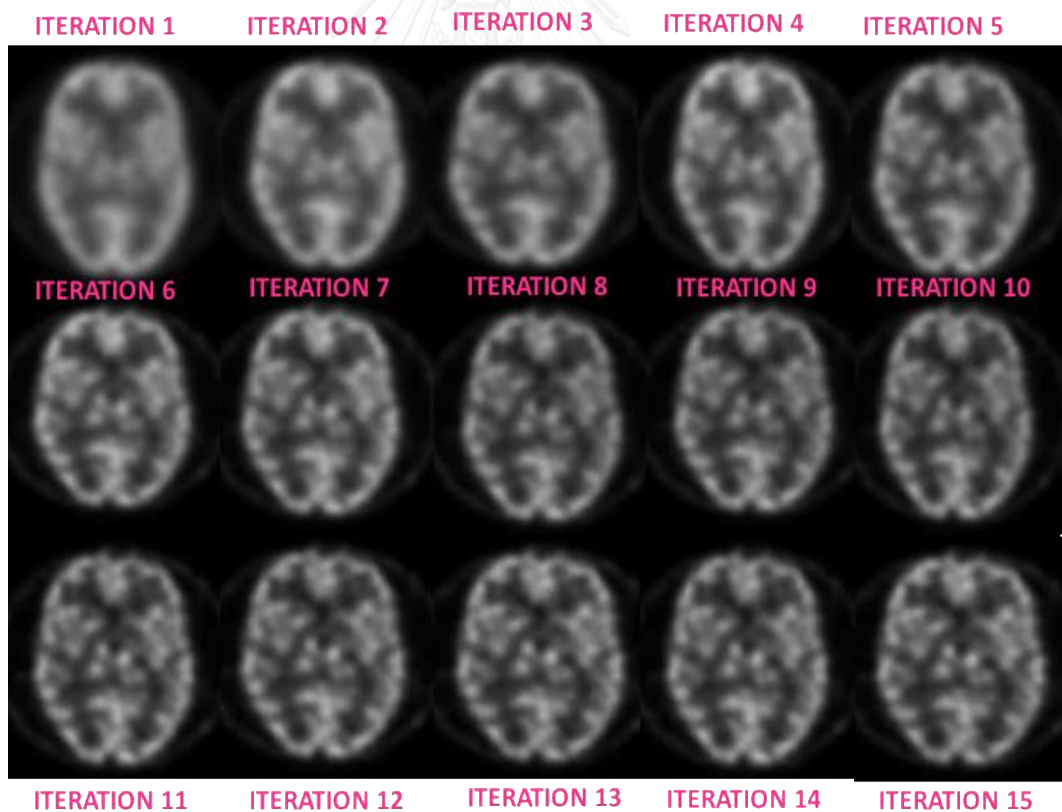


Figure B 3. The brain SPECT images by varying number of iterations in normal activity concentration (3D- OSEM)

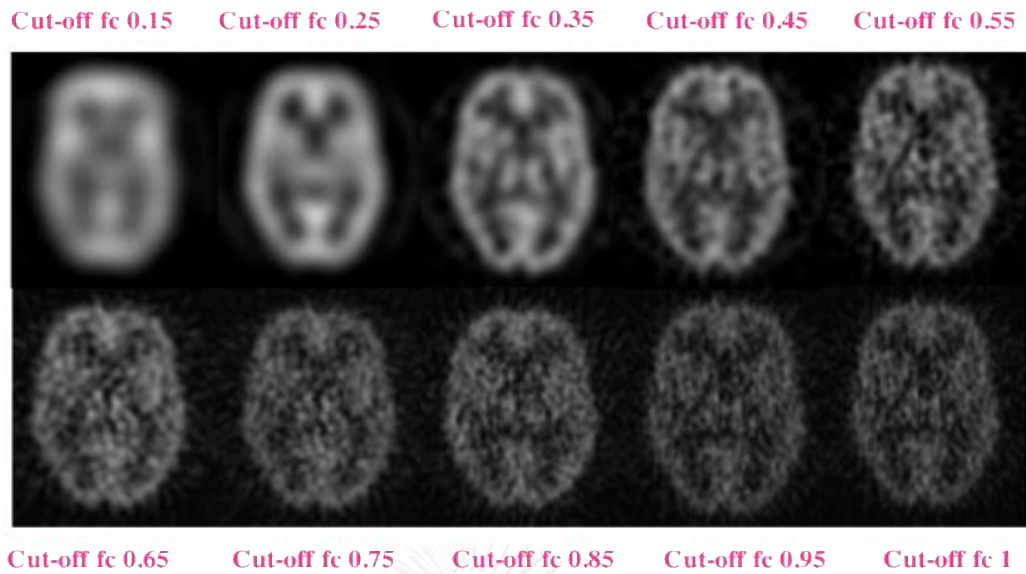


Figure B 4 The brain SPECT images by varying cut-off frequencies in normal activity concentration (FBP method)

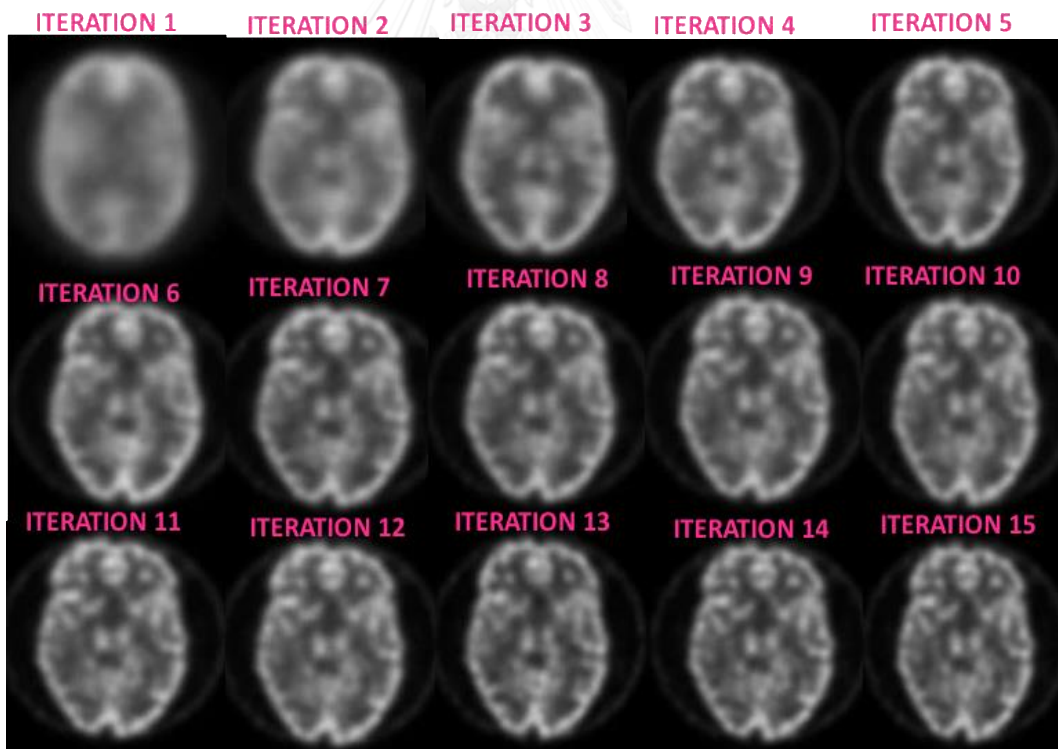


Figure B 5. The brain SPECT images by varying number of iterations in high activity concentration (3D- OSEM)

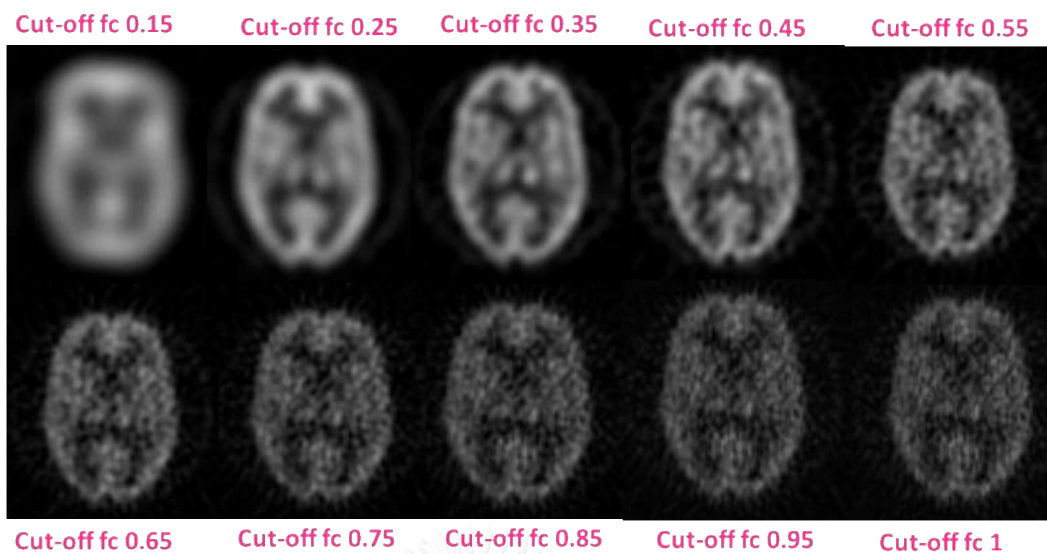
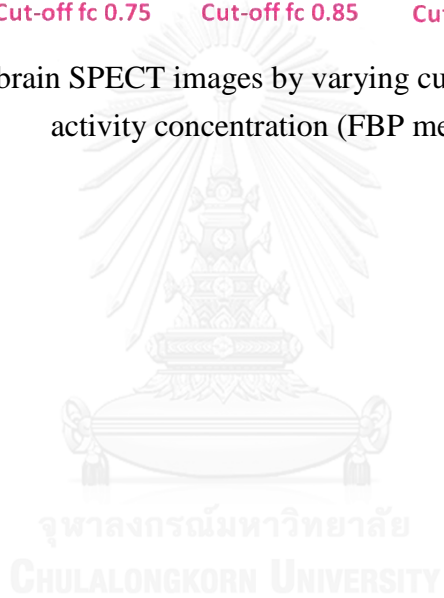


Figure B 6. The brain SPECT images by varying cut-off frequencies in normal activity concentration (FBP method)



VITA

Name	Miss May Phyu Zin Thein
Sex	Female
Nationality	Myanmar
Date of birth	7. May. 1987
Place of birth	Yangon
Institution	University of Medical Technology (Yangon-2007)
Address	Room No.2104@MDCU apartment, Chulalongkorn Hospital, Bangkok, Thailand. Tel. 0839634454
E-mail	mmphyuzin87@gmail.com